RSC Advances

REVIEW

View Article Online
View Journal | View Issue

Cite this: *RSC Adv.*, 2021, **11**, 13674

Gold-carbonaceous materials based heterostructures for gas sensing applications

Sanjay Kumar,[ab] Suneel Kumar,[c] Manisha Sengar[d] and Pratibha Kumari *[a]

There is a growing and widespread interest in developing powerful gas sensors to track the level of environmental pollution by detecting the unintended release of poisonous gases into the atmosphere; the gas sensing devices prevent endangering human life as well. Due to their large surface area, more active adsorption sites, high electron mobility, hollow structure, and physicochemical stability, carbon-based nanostructured materials such as carbon nanotubes (single and multi-walled carbon nanotubes) and nanowires are promising gas sensors. The surface modification of carbon nanostructures with gold nanoparticles increases sensitivity and sensing response time, and it is possible to produce a process that is operational at room temperature. Gold nanoparticles' astounding role coated on carbon nanomaterials in hole mobility modulation renders them the most promising candidate for gas sensing applications by acting a nano-Schottky barrier. An overview of recent developments in carbon nanostructures decorated with gold nanoparticles, their gas sensing applications, and the mechanistic point of view has been summarized in this review.

Received 15th January 2021
Accepted 27th February 2021

DOI: 10.1039/d1ra00361e

rsc.li/rsc-advances

1. Introduction

In the past decade, gas sensing has emerged as a superior technique for sustainable development and has been an intense research subject in the scientific community.[1] The gas sensing application is highly advantageous in various industries to detect the leakage of harmful gases. The ideal concentration of environmental gases is also ensured by proper monitoring through analyzing and sensing techniques. Most importantly, astronomers need better gas sensing techniques for exploring the ecological conditions of different planets.[2] The worldwide use of gas sensors necessitates the exploration and fabrication of nanomaterials for sensing applications.

A gas sensor must have high sensitivity and selectivity toward gases, prompt response, fast recovery time, temperature independence, and cost-effectiveness. The gas sensors include

[a]*Department of Chemistry, Deshbandhu College, University of Delhi, New Delhi-110019, India. E-mail: pratibhatanwar77@gmail.com*
[b]*Department of Chemistry, University of Delhi, New Delhi-110007, India*
[c]*Department of Chemistry, Government Degree College Chamba, Sultanpur, Chamba, Himachal Pradesh, India*
[d]*Department of Zoology, Deshbandhu College, University of Delhi, New Delhi, India*

Mr Sanjay Kumar is currently pursuing his PhD degree under the supervision of Dr Pratibha Kumari from University of Delhi, India. He received his MPhil., MSc, BSc, degree in Chemistry from Himachal Pradesh University, Shimla, India. His main area of interest entails material chemistry and supramolecular nano assemblies and their exploitation in environmental science.

Dr Suneel Kumar is currently working as an Assistant Professor (Chemistry) at Government Degree College Chamba, Himachal Pradesh, India. Dr Kumar received his PhD degree from Indian Institute of Technology (IIT) Mandi, India in 2019. Previously, he received his BSc and MSc degrees in chemistry from Himachal Pradesh University, Shimla in 2011 and 2013, respectively. His main research interest is in the field of semiconductor and two-dimensional materials based photocatalysis for energy conversion and environmental remediation applications.

various semiconductor materials, mainly metal oxides such as WO,[3] TiO_2,[4] ZnO,[5] and polymeric materials.[6] Porous material has also been widely explored for gas sensing technologies due to effective adsorption and gas molecules' desorption onto their surfaces.[7] The contact between the analyte and the sensing material is a crucial factor for determining the sensitivity of the techniques. Hence, porous structures and hollow spaces are preferred over flat surfaces for gas sensing application. With the nanotechnology advancements and the introduction of nanomaterials such as nanospheres, nanotubes, nanofibers, and nanowires, significant progress has been observed in the sensing field. It is noteworthy to mention here that, to obtain high-performance devices, a high operating temperature is required, which limits their applications. Therefore, the design and development of cost-effective, selective, portable, and highly sensitive gas sensors which can work at low temperature are highly anticipated.[8]

The development of various nanomaterials is gaining towering height due to their unique properties and wide applications.[9–16] Recently, carbonaceous materials such as graphene, carbon nanotubes (CNTs), graphitic carbon nitride have attracted enormous attention due to their excellent physical, chemical properties, high specific surface area, *etc.* Furthermore, carbon nanomaterials' mechanical properties increase their suitability to integrate them into flexible sensor devices.[17] The robust nature of these materials also offers selective and sensitive fabrication by employing different techniques to create defects and grafting functionalities onto their surfaces in a controlled way. Carbon nanomaterials include versatile type's morphology such as nanofibers, nanosheets, and various nanotube materials. Carbon nanotubes (CNTs) are among the much explored carbonaceous materials for gas sensing applications, followed by graphene.[18,19] After their discovery in 1991, the carbon nanotubes have been well studied concerning their geometry, morphology, electrical properties, mechanical and optical properties.[20] Carbon nanotubes (CNTs) are classified under fullerenes structures and broadly divided into two types, namely single-walled carbon nanotubes (SWCNTs) and multi-walled carbon nanotubes (MWCNTs). SWCNT is a one atom thick structure with a cylindrical shape with a nanoscale diameter, but the length may vary in microns.[21]

On the other hand, MWCNTs are multiple graphite layers wrapped like a tube and sharing the same central axis.[22] The properties of CNTs are inherently smart such as mechanical strength, stiffness, and electrical properties, depending upon tube diameter and chirality. They are highly anisotropic because of the one-dimensional structure enabling high charge carrying capacity.[23] Structural elucidation of CNTs comprises achiral-armchair type, achiral-spiral type, and chiral or helical structures.[24] CNTs find multiple applications in the fields of telecommunication, energy conversion, energy storage, biological sensing, catalysis, nanoprobes, nanoelectronics, and coating and filling materials, *etc.*[25–28]

Interestingly, the chemiresistor and chemical field-effect transistors-based gas sensors are most promising owing to their excellent electrical properties of nanostructures. The electrical properties of CNTs change dramatically when their surface is exposed to target analyte gas. The transfer of electrons between the two moieties is the basis of change in electrical properties. Hence, factors that enhance the adsorptive interactions between the gas molecule and CNT surface result in better sensing results.[29] In addition to CNTs, the carbonaceous material, particularly graphene, has been widely investigated for gas sensing applications because of its fascinating electronic properties such as zero bandgaps, ultra-fast electron mobility, and outstanding thermal conductivity (5000 $W\ m^{-1}\ K^{-1}$). Ideally, graphene is one atom thick two-dimensional layer of sp^2 hybridized carbon atoms with a high comb-like lattice structure.[30] The high specific surface area and easy exfoliation techniques of graphene lead to its wide use in the fabrication of gas sensing devices.[31]

Various metal nanoparticles nanocomposites with CNTs to form resistance-based gas sensors have been extensively

Dr Manisha Sengar completed her graduation and post-graduation from the University of Delhi, India. She did her PhD from Grain Technological Institute, Kanpur, India. Presently, she is working as an Associate Professor in the Department of Zoology, Deshbandhu College.

Dr Pratibha Kumari has been working as an Assistant Professor in Chemistry at Deshbandhu College, University of Delhi, New Delhi, India. She received her BSc, MSc, MPhil and PhD degree in the field of Chemistry from University of Delhi, New Delhi, India. She extensively worked on green synthesis, catalysis and sensing applications of macrocyclic molecules. She also worked as a visiting Assistant Professor (INDO-US fellow) at San Diego State University, California, USA in 2020 on energy applications. Her current research interests mainly focus on catalysis, sensing, nanomaterials, medicinal chemistry, energy conversions, and supramolecular chemistry.

reported in the literature with enhanced selective/specific sensing output compared to pristine CNTs.[32–34] Out of various metal nanoparticles, Au nanoparticles (Au NPs) beg a special place owing to their broad application and peculiar plasmonic properties. Au is one of the most valuable discoveries in ancient times, and Au NPs are of paramount interest to the scientific community in this century. Au NPs are the most stable metal nanoparticles and are illustriously used in electronics, catalysis, and the medicinal field.[35,36] The metal nanoparticles where properties crucially depend upon size show interesting quantum effects. There are several reasons responsible for the extensive use of Au NPs for various technological applications; (i) high chemical and physical stability and biocompatibility of nanoparticles in physiological condition, (ii) the presence of polarizable electrons on NPs surface leading to optical activities such as surface plasmon, and (iii) easy functionalization possibility with other substrates. In addition to the properties mentioned above, Au NPs also show excellent chromophoric effect due to their more significant extinction cross-section. The surface plasmon resonance (SPR) property is associated with free-electron oscillations on metal surfaces under the impact of electromagnetic radiations. However, excitation of plasmon by an electric field is not allowed in the bulk matter because of energy limitations.[37,38] These surface plasmon properties often serve as a probe to monitor the bonding interactions between surface and adsorbed molecules. The conductive surface further facilitates the adsorbed gas molecule toward selective redox processes.[39] Hence the role of Au NPs becomes more climacteric in the fabrication of nanosensors for the detection of gases.

Therefore, keeping in mind the properties mentioned above of Au NPs and carbonaceous materials, particularly CNTs and graphene, we have focused this review on the recent progress in gas sensing application of Au-carbonaceous materials-based heterostructures. Furthermore, we have discussed various fabrication strategies of CNTs for gas sensing devices, followed by a comprehensive summary of the recent reports based on Au-CNTs heterostructures. Additionally, the fundamental sensing mechanism of the gas sensor has been systematically discussed. Finally, the challenges and further possibilities for the development of high-performance gas sensing devices have been discussed.

2. Preparation of carbonaceous materials for gas sensing

Carbon-based materials are relatively much used in sensing technology, including biosensing,[40] chemical sensing,[41] gas sensing[42] *etc.* In gas sensing application, CNTs and graphene have been utilized the most due to their unique properties. Therefore, an overview of their synthetic methodologies is crucial for the development of carbon-based promising materials for gas sensing.

2.1 Preparation of CNTs

There are various methods for the preparation of CNTs for the fabrication of gas sensing devices. In this section, we have discussed some of these important preparation methods in detail. Some of the common techniques such as chemical vapour deposition (CVD), laser ablation, electric arc, liquid electrolysis, and plasma torch are extensively used in the fabrication of CNTs. The different methodologies were adopted to produce CNTs with different electrical and mechanical properties. The semiconducting and metallic nature of CNTs is also affected by different fabricating techniques. The techniques also result in varying lengths of tubes, consequently leading to affect the application. Fig. 1 shows the different methods adopted for the preparation of CNTs.

The electric arc discharge method has been used in the early '90 s for the development of fullerenes. Iijima also discovered CNTs using the same process in 1992.[43] An electric arc produces high temperatures under an inert atmosphere in a typical procedure, and carbon atoms are generated from the carbon source (carbon electrodes). Helium (He) gas, used for inert atmosphere, increases carbon deposition during the process. The amount of carbon deposited on the cathode by applying a high voltage arc depends on He gas's pressure. The size of the diameter of anode and cathode are also playing a crucial role in the synthesis of CNTs. Generally, anode diameter size was kept smaller than the cathode and observed that increased electrode diameter cause sintering and cracking of CNTs.[24] The laser ablation technique uses intense laser pulses in a vertical chamber in inert gas, like argon and catalyst, to produce CNTs and nanomaterials. The technique uses high temperature like the arc discharge method but remains the most popular method for the production of CNTs commercially. An improved laser ablation method reported in 1995 at Rice University used a double-pulse laser oven process.[44] Laser wavelength used for ablation ranging from 193 nm (ArF laser) to 10.6 μm (CO_2 laser) and also observed that shorter wavelengths in ultraviolet light predominantly produce MWCNTs while larger wavelengths near the IR region produce SWCNTs.[45] The chamber's properties used in pulse laser deposition, such as oscillation wavelength and peak power, also affect the properties of the grown CNTs. The plasma torch is a relatively newer technique to produce CNTs from graphitic material in the presence of catalysts on silicon-based substrates. The microwave plasma torch of power 2.45 GHz at atmospheric pressure is used to decompose the precursor in the presence of a catalyst. In one example, the authors described the formation of MWCNTs using CH_4/H_2/Ar on the silicon substrate. The iron oxide NPs used as a catalyst in the process obtained from the decomposition of $Fe(CO)_5$. The method successfully produced well-aligned CNTs at atmospheric pressure without external heating.[46,47]

Nevertheless, electrochemical methods are trendy in the preparation of carbon-based nanomaterials. Electrolysis is a method which involves molten salts to produce CNTs by decomposing CO_2 by electrochemical reactions under excess pressure. This is the most straightforward technique used in CNT production due to simple apparatus, low energy requirements, and controlled synthetic strategies. Chen *et al.*[48] reported the electrolytic conversion of graphite to CNTs in molten alkali chlorides (LiCl, KCl, NaCl). The CNTs were obtained at the cathode, where an electrolytic reaction took place to form alkali metal. The CNTs were obtained from the crucible containing a cathode, and the highest yield was reported in the case of

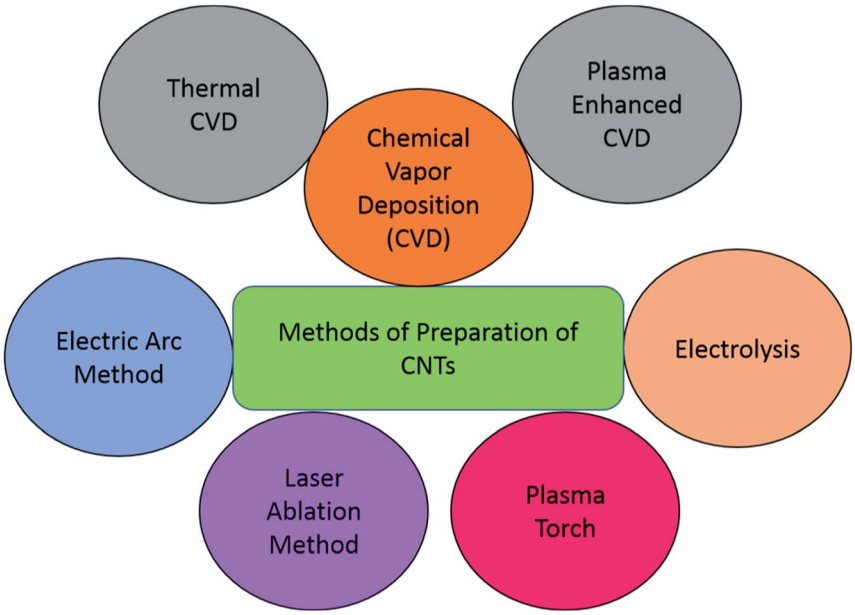

Fig. 1 Diagrammatic illustration of different methodologies adopted for obtaining CNTs.

NaCl. The CVD method, employed to CNTs production from the vapor state of carbon, and therefore, various techniques to vaporize the carbon materials are reported in the literature.[49] The CVD system is one of the methods in which hydrocarbons are broken in a reaction chamber at elevated temperatures (550–1000 °C) in the presence of a catalyst.[50]

The two primary techniques used in the CVD method are thermal CVD and plasma-enhanced CVD. Jung *et al.*[51] reported Ni nanoparticles' use as a catalyst in the CVD growth of CNTs. The CNT growth behavior was observed in the environment of H_2, N_2, NH_3, Ar, and their mixture. The pure N_2 environment leads to the deposition of the carbon layer on the substrate and encapsulates Ni, which could not act as a catalyst; hence CNT growth deferred. On the other hand, in pure H_2 and NH_3, randomly tangled CNTs and vertically aligned CNTs were obtained, respectively.

Relatively low-temperature production of CNTs using the plasma-enhanced CVD method gain much popularity where Fe or Co was used as a catalyst.[52] In similar studies, Favvas *et al.*[53] reported the preparation of phenol functionalized MWCNTs using a fluidized chemical bed CVD vertical reactor. In CVD, commonly, there are two-step processes involving the use of carbon-containing gas and process gas. The carbon-containing gas is broken down at the surface of the nanoparticle catalyst, and the nature of the CNT generation depends upon the nature of the process gas and the size of the catalyst. There are many other types of CVD methods previously applied to obtain CNTs, such as oxygen-assisted CVD, radio frequency, and hot filament CVD.[54,55] Resistivity vaporization of graphite and vaporization carried out by electron or ion beam were also reported in the literature.[56,57]

2.2 Preparation of graphene

Graphene is an allotropic form of carbon which is consists of sp^2 hybridized carbon atoms and has honeycomb like structure. Graphene is a versatile and upcoming material owing to its high intrinsic mobility, conductivity and Young's modulus and optical transmittance. Graphene and graphene oxide based materials have been explored for sensing applications. There are various synthetic methods for the synthesis of graphene and graphene oxide, primarily, utilizing the top-down approach.[58] The mechanical exfoliation has been a very easy and simple approach to synthese graphene. Electrochemical exfoliation has also been developed for more production efficiency and high purity graphene material. Intercalation in graphite is another approach to produce graphene using intercalation compounds which causes the increase in the distance of interlayers. Pyrolysis is a very easy method but the product so obtained is not of high purity which limits applicability of this method. Graphene oxide is the monolayer form of graphite oxide which also has versatile application in environment and energy. There are many report on synthetic methodologies of graphene oxide which involves the oxidative exfoliation of graphite using strong oxidizing agent.[59] Hummer method, modified Hummer method and improved Hummer method are the most commonly used methods to prepare graphene oxide.[60–62]

3. Application of carbonaceous materials in gas sensing

3.1 CNTs as gas sensors

As this is well reported in the literature, the large tubulene surface area is the first vantage coin for sensing application. High adsorption capacities and towering sensitivity of CNT accommodate atoms and molecules on their surface and furnish the possibilities of designing sensors. CNT gas sensors depending upon the mode of action have been classified as (i) ionization gas sensors, (ii) gas sensors based on sorption, (iii) gas sensors based on capacitance, and (iv) gas sensors based on

resonance frequency shift.[18,28] Ionization gas sensors use CNTs as electrode materials, and gas ionization parameters are determined during accelerated ion collision with gas molecules. Although the working voltage required is very high, ionization sensors are less accessible among sensing techniques.[63] Hui *et al.* demonstrated the tripolar electrode ionization sensor based on CNT cathode to determine nitric oxide. The method is more useful where the adsorbing capacity of gas molecules is low.[64]

However, sorption-based gas sensors are commonly used in sensing technologies. The basic principle behind these sensors is the gas molecule's adsorption onto the surface of either pristine CNTs or fabricated CNTs with metal oxide nanoparticles, polymers, or other functional groups. The mechanism involves transferring an electron between adsorbed atoms or molecules and the CNT surface, which subsequently changes nanotubes' electrical properties and conductivity.[65] Mehdi *et al.* confirmed the charge transfer in intermolecular interactions through atoms in molecule theory and natural bond orbital calculations for sensing N_2O gas molecule on Pd/CNT surface.[66]

The capacitance-based gas sensors use CNTs as sensitive materials. In such a typical gas sensor, a layer of CNTs grown over the layer of SiO_2 and vapors of a gas molecule adsorbed on the layer's surface get polarized when an external voltage is applied due to an electric field generated on the surface of CNTs.[28] This led to a change in capacitance values. Generally, the capacitance signal is sensitive to gas molecules' relative humidity.[67,68]

The electrical properties of CNTs play a substantial role in sensors based on resonance frequency shift. The change in electrical properties on the gas molecule's adsorption on CNTs is the fundamental principle behind these sensors. The sensitive element in these sensors includes disk resonators with nanotubes grown on their surfaces. When gas molecules interact with the surface of CNTs, the dielectric permeability of the disk changes, consequently shifting the resonance frequencies. The frequency shifts are different for different gas molecules; therefore, these sensors are more selective than others.[69]

The surface properties of CNTs and their interaction with different electron-withdrawing/donating groups result from changes in conductance values, which is the basis of sensing application. Despite having several merits, pristine CNTs have specific limitations such as lesser selectivity, larger recovery time, and lower sensitivity toward gas analytes that are not strongly adsorbed or interact with the surface. The sensing platform's recovery is crucial, which is even impacted by the stronger analyte interactions with CNT surface and making desorption more difficult.[70] Many researchers have fabricated and functionalized the CNTs to overcome the limitations and enhance the sensitivity and selectivity toward gas analytes. Many attempts have been made to enhance the sensor performance by functionalizing CNTs with polymers,[71] metal oxides,[72] and various other catalytic materials.[73,74] The functionalization of CNTs can be done with various other metal nanoparticles, but this review explicitly emphasizes the heterostructures of CNTs with Au.

3.2 Graphene for gas sensing application

As discussed in the earlier section that, graphene exhibits fascinating properties such as high specific surface area, excellent thermal conductivity, high Young's modulus, fast electron mobility, *etc.*, which makes it a unique material. Till date, many research groups have utilized this interesting material for a variety of technological applications such as chemical sensors,[75] field-effect transistors (FETs),[76] Li-ion batteries,[77] supercapacitors,[78] energy storage,[79] molecular imaging,[80] biomedical applications,[12,81] and catalysis.[82] Recently, graphene-based materials have been widely employed in gas sensing, particularly due to a large specific surface area provided by its 2D honeycomb-like lattice structure.[83] The first breakthrough in gas sensing by using graphene came in 2007 by Schedin *et al.*[84] in this work, the authors demonstrated that the adsorbed gas molecules increased the graphene's charge carrier density. Following this work, various research groups devoted their studies to exploring the graphene-based materials for gas sensing.[31] Furthermore, the functionalization of graphene to form graphene oxide (GO) has turned one of effective strategy to enhance the sensing performance of device. It has been reported by Tang *et al.*,[85] that the functionalization of graphene leads to the stronger interaction between gas molecules and surface as compared to pristine graphene. The presence of various facile and well-explored GO preparation methods from graphene has drastically increased GO's utilization as an interesting sensing material. The removal of oxygen-containing functional groups obtains another form of graphene to rejuvenate the π conjugated structures. This is a reduced form of graphene and is known as reduced graphene oxide (rGO). The rGO can be obtained by chemical reduction, thermal reduction and by electrochemical production method.[86] The high electrical conductivity and exposed defect sites in rGO make it an ideal material for gas sensing. Therefore, there are many reports in literature in recent years wherein graphene, GO, and rGO have been utilized to fabricate gas sensing devices.[31,72,87] Most importantly, both GO, and rGO can be easily synthesized from precursor material graphite compared to graphene. Moreover, in order to further improve the performance and selectivity of gas sensing devices, the GO, and rGO has been decorated with metal nanoparticles to from heterostructures.[72,88–90]

Prezioso *et al.*[91] have reported a low-cost, highly sensitive gas sensing device fabricated by drop-casting method on standard interdigitated Pt electrodes. The entire fabrication process of gas sensing device based on single-layer GO flakes and interdigitated Pt electrodes has been depicted in Fig. 2. Besides, the SEM images in Fig. 2 presents the electric contact between GO flakes and Pt electrode. The prepared device exhibits an excellent lifetime of more than 1000 s and a very low detection limit of 20 ppb for NO_2 gas at different temperatures and gas concentrations. This GO-based gas sensing device's remarkable performance has been attributed to GO flakes' excellent quality with abundant active sites over its surface. The GO surface's active sites mainly contain various functional groups such as hydroxyl, carbonyl, *etc.* These functional groups help in the adsorption of NO_2 molecules, which increases the binding energy and facilitates the charge transfer from NO_2 to GO, resulting in the chemisorption of gas molecules.

In another work by Lu *et al.*,[92] the exceptional properties of rGO have been exploited for the fabrication of a chemical

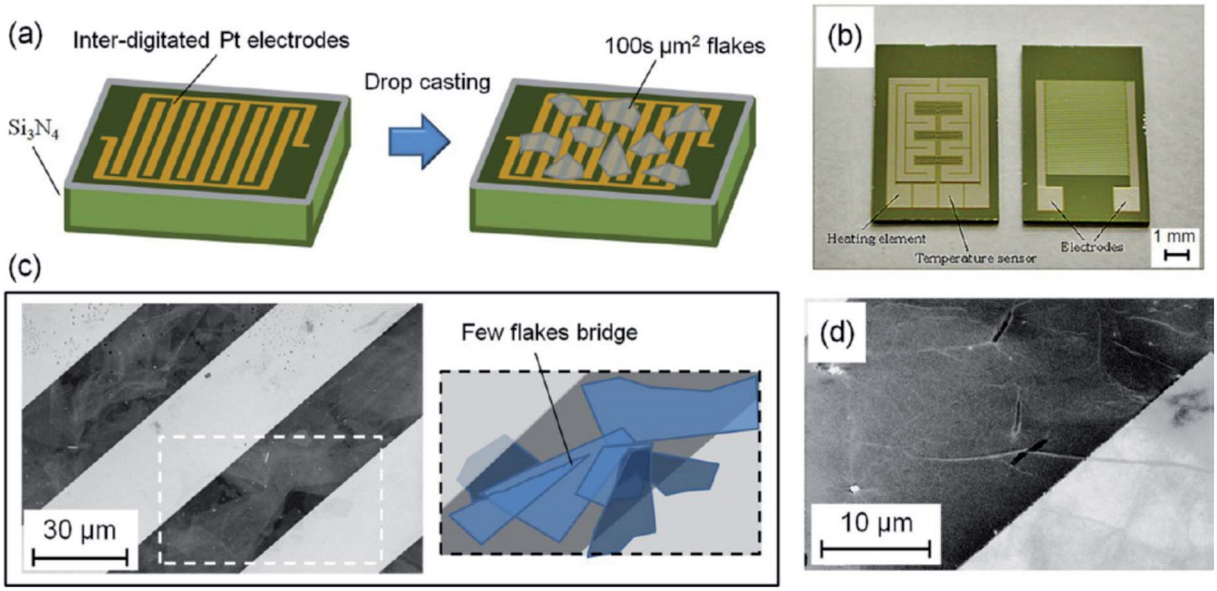

Fig. 2 (a) Schematic depicting the device fabrication, (b) patterned substrate (front-size) with heating elements and temperature sensors on the backside. (c) SEM image of few GO flakes bridging two adjacent Pt electrodes. (d) SEM image of a GO flake lying over an electrode edge. "this figure has been adapted/reproduced from ref. 91 with permission from American Chemical Society, copyright 2013".

sensing device. The graphene was reduced chemically using hydrazine monohydrate to form rGO platelets as one of the conducting channels on a field-effect transistor (FET) platform. Furthermore, fabricated devices have shown high sensitivity and excellent response towards low concentrations of NO_2 and NH_3 gases in the air. Such a remarkable sensing response has been attributed to the facile charge transfer between rGO and target gas molecules. This work has also been supported by the theoretical analysis, which provides insightful information about signal processing methods to fabricate graphene-based chemical sensing devices.

Despite the various attractive properties of graphene-based materials in gas sensing, the low selectivity of GO and rGO based sensing devices remains a bottleneck for their practical applications. Lipatov *et al.*[93] have addressed this issue by reporting an array of rGO based integrated sensors. In this array, the nanoscale to microscale rGO films has been utilized, which results in the excellent response of each variety in an integrated device. The variable structure on rGO films enables the interaction between analyte molecules and fabricated sensors due to similarity in chemical structure. Such chemical interaction imparts excellent selectivity to sensors towards methanol, ethanol, and isopropanol.

4. Gold nanoparticles in gas sensing

Due to the unique photosensitive properties, Au NPs are being studied for their application in optical sensing devices over the decades. Tremendous work has been done to modify the properties of Au NPs for sensor development, including gas sensing. Most of the work reports Au NPs for the detection of different target gases by combining them with other materials. Kawaguchi *et al.*[94] reported that the sensing performance of immuno-surface increased four-folds when modified with Au NPs. Gallium nitride nanowires were functionalized with Au NPs for sensing argon, nitrogen, and methane.[95] The Au NPs, combined with TiO_2, were investigated to detect alcohol vapors and gases.[96] Borhaninia *et al.* synthesized SnO_2 nanoparticles using the sol–gel method by mixing with different amounts of Au NPs for sensing carbon monoxide.[97] Naama *et al.*[98] investigated silicon nano-wire modification response with Au and Pt NPs as CO_2 gas sensors and shown that the sensor's performance depends upon the type of metal nanoparticle. Recently, Au NPs of different shapes and sizes were incorporated in the mesoporous silicon layer to be used as CO_2 gas sensors.[99] In recent work, it was explored that Au NPs deposited on the surface of ZnO microstructure gave better gas response towards ether than pure ZnO microstructures.[100] The gas response was shown to be increased with an increase in temperature. A hybrid of ZnO nanowires functionalized by Au NPs was synthesized for gas sensing applications. The sensing performance of the hybrid was analyzed and compared with that of the pure ZnO sensor. Improved response and higher selectivity were observed that might be attributed to the increased Schottky barriers caused by the electronic interaction between Au NPs and ZnO nanowires.[101]

Apart from Au NPs, the complexes of Au are also demonstrated for gas sensing applications. In such examples, an Au(III) pincer complex was synthesized and operated at room temperature for selective and sensitive detection of NH_3 gas.[102] The cyclometalated alkynyl-gold(III) complex was recently used as a fluorescent film for sensing ketones in the vapor phase.[103] The surface plasmon resonance effect of thin films or NPs of Au could also be utilized in sensing response to different gas analytes.

Furthermore, Au NPs have also been used with different polymers for sensing different gases. Hydrogen sulfide gas has been efficiently detected using bio-functionalized Au NPs. It was

reported that sensing performance might be due to bio-moieties with high dielectric constant.[104] In another study, Au NPs have been functionalized with a special polymer to detect dissolved carbon dioxide.[105] Further, several reports are available on the potential of Au NPs as a sensing platform for the detection of volatile organic compounds. Xie *et al.*[106] investigated that the sensitivity and selectivity of Au NPs for acetone and other volatile organic compounds which got improved when Au NPs are functionalized with thiol monolayer. Daskal *et al.*[107] reported the fabrication of thin-film composites of Au NPs on a silicon wafer using different organic linkers to detect volatile organic compounds. *In situ*-decorated with Au NPs on the surface, a three-dimensional tin dioxide nanostructure exhibited high gas sensing performance with high selectivity towards volatile organic compounds.[108]

Yunnan Fang *et al.*[109] demonstrated the inkjet-printed interdigitated electrodes (IDEs) on SWCNTs fabricated with Ag followed by conversion to a highly porous Au counterpart. The resulting porous Au IDEs possess a five-time higher sensitivity than the Ag counterpart without losing the substrate-IDE adhesion. The flexibility and mechanical robustness in sensor devices and enhanced capacitance and electrical conductivity of CNTs achieved through electrochemical deposition of Au NPs on CNT transducers. The hybrid nanomaterials could be utilized in the wearables.[110] Various synthetic strategies were adopted to obtain hybrid nanostructures based on the Au and CNTs to overcome the limitations incurred during pristine analog for obtaining better sensing performance. The functionalization of CNTs also enhances the electrical properties, lower recovery rates, increased selectivity, and mechanical robustness. This report focuses on selected Au and carbon-based heterostructures, their synthetic strategies, and their exploitation in various gas sensing applications.

5. Gold-carbonaceous heterostructures for gas sensing applications

5.1 Gold-CNTs nanostructures

Fabrication of nanocomposite materials and their engineering and mechanism control improve the overall activity of heterostructures. The CNTs-Au NPs heterostructure is fabricated through controlled approaches where AuNPs are grown on or inserted inside the cavities of CNTs. The assembly of composite material where Au NPs are incorporated inside of CNTs depends upon host–guest chemistry. The interior surface of CNTs is relatively inert, with a diameter size ranging from 1–50 nm. The strong interaction between Au NPs and CNT is anticipated based on appropriate measures. If the CNT diameter is too big or small compared with the van der Waals diameter of guest molecules, interactions are weaker.[111,112] We have discussed in detail about CNTs-Au heterostructures fabricated through various gas sensing applications in the subsequent sections.

A method for filling up MWCNTs with Au NPs involves using the aqueous citric acid solution and nanotubes heated in the ammonical environment. The heating of MWCNTs in NH_3 opens the ends of nanotubes and creates basic groups on inner walls. However, citric acid interacts with basic groups through electrostatic interactions and reduces Au NPs inside the MWCNTs.[113] Andrei N *et al.*[114] reported the Au NPs encapsulation inside MWCNTs with supercritical CO_2 process. The growth of Au NPs inside the tube was explained based on Ostwald ripening,[77] where thermodynamic parameters lead to larger NPs at the cost of smaller ones with time. The shorter length of nanotubes is desired to overcome the transport resistance of nanoparticles inside the tube, and Au NPs enter either through-hole or open end of the tube. The author explains the pyrolytic cutting of CNTs with metallic silver acting as a catalyst and generated from $AgNO_3$ (shown in Fig. 3). The Au NPs first adsorbed onto the surface of CNTs and then transferred and encapsulated inside the tube.

5.1.1 Direct assembly of Au NPs with carbon nanotubes. Functionalization of CNTs surface is necessary to fabricate Au NPs onto them. Various research groups reported functionalization of CNTs surface with multiple groups such as bifunctional thiols,[115] polyelectrolytes,[116] Electrochemical modification,[117] diimide activation,[118] and microwave-assisted modification and fabrication of Au NPs on the surface of CNTs.[119] However, modification of CNTs done by grafting various functional groups at the tip, replacing some of the atoms on the tube with other, and intertubular spaces can accommodate guest molecules. Thermal

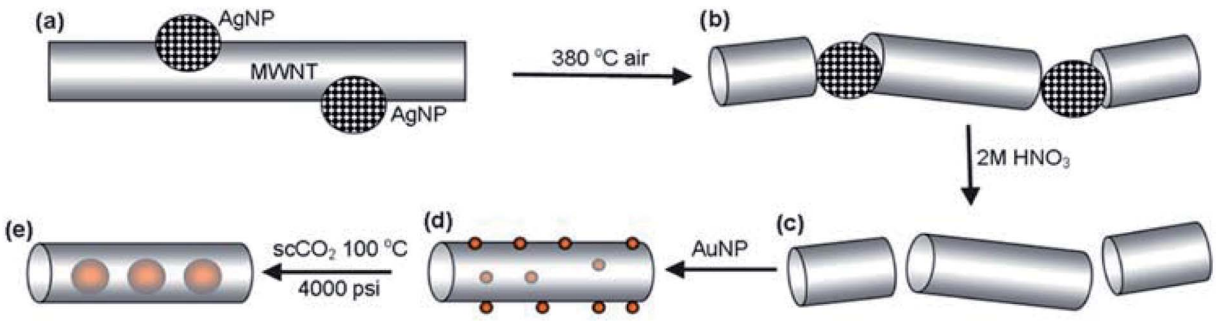

Fig. 3 Scheme showing the proposed mechanism for filling CNTs with Au NPs (a) Ag NPs thiol stabilized on nanotube surface, (b) Ag NPs catalyzed pyrolysis of CNTs, (c) short and open-end nanotubes, (d & e) discrete surface adsorbed Au NPs (red balls) "this figure has been adapted/reproduced from ref. 114 with permission from Royal Society of Chemistry, copyright 2009".

deposition of Au NPs on the surface of nanotubes is the ubiquitous physical method. Bühlmann *et al.*[120] reported the thermal evaporation method for deposition of Au NPs on MWCNTs. The MWCNTs were prepared by the chemical vapor deposition (CVD) method, and the size of the deposited particle depends upon nominal film thickness.[120] Another research group also reported a high vacuum chamber for thermal deposition.[121] Adsorption of Au NPs carried out on the surface of CNTs carried out by redox reactions where solid support like SiO_2 utilized. Notably, the condition of imposing high temperature and use of linker aborted.[122]

Nevertheless, in these methods, an informal distribution of Au NPs not assured and are not soluble due to solid support material. Geckeler *et al.* reported a similar water-soluble hybrid material approach where SWCNTs hole-doped with Au NPs.[123] They used the solution phase dispersion technique where metal nanoparticles were obtained by mixing metal salt with surfactant suspended nanotubes in water. Frontier orbital picture analysis confirms the uniform distribution of Au NPs on side walls of nanotubes. There are many reports on direct deposition of metal NPs on surface of CNTs through various techniques such as electron beam deposition,[124] solvated metal atom dispersion method (SMAD),[125] wet chemical methods.[126–128]

5.1.2 Au NPs assembly with carbon nanotubes with linker. The adsorption of Au NPs by the direct assembly on CNTs generally carried out by adopting *in situ* methods that do not give better uniform distribution results. Moreover, sensing devices must have a broad range of working conditions, and hence assembly of nanomaterials must sustain severe conditions. The Au NPs adsorbed through the linker on the surface of CNTs overcomes these conditions. The linkers used for this purpose further divide into two categories, (i) non-covalently linked nanocomposite and (ii) covalently linked nanocomposites. Covalent linkage established between Au NPs and functionalized CNTs with activated groups like carboxylate groups,[129] thiols,[115] cysteamine,[130] and aryl group,[130] *etc.* Recently, Baoshan *et al.* developed an aptamer sensor for the detection of sulfadimidine (SM2). 2-Aminoethanethiol (2-AET) is used as a linker between Au NPs and MWCNTs surface in this work. In a typical procedure, bare Au electrode first functionalized with 2-AET and further established an amidic bond between aminic groups of 2-AET and carboxyl groups of MWCNTs immobilized MWCNT/Au NP nanocomposites.[131] While, non-covalent functionalization of Au NPs with CNTs were reported based on π-stacking interactions,[132] hydrophobic interactions *e.g.*, sodium dodecyl sulphate,[133] and electrostatic interactions *e.g.*, poly(diallyldimethylammonium chloride).[134,135] Coleman *et al.*[129] reported the Bingel addition for the fabrication of SWCNTs surface with Au colloids. In a typical procedure, SWCNTs have taken in dry *ortho*-dichlorobenzene (*o*-DCB) and 1.8 mmol of diethyl bromoanalate and 3.3 mmol of 1,8-diazabicyclo[5.4.0]undecene (DBU) added to get modified SWCNTs [$(COOEt)_2C <$ SWCNTs]. The immobilized modified SWCNTs onto Si substrate further trans-esterified with an excess of ethanol. The 5 nm Au colloids are exploited through Au sulfur linkage with a chemical tagging procedure.

The 1D materials, due to their remarkable properties also reported by Wu *et al.*,[136] where SWCNTs were used as the template for assembling Au NPs linear arrays. The process involves functionalizing SWCNTs with bovine serum albumin (BSA) protein to obtain BSA-sheathed SWCNTs. Au NPs obtained the linear array due to Au-thiol linkage with BSA on SWCNTs followed by electroless metal deposition to form a 1D linear array. The rigid superstructure nanowires obtained can be changed in morphology by changing the concentration of precursor material. Recently, Michael *et al.*[137] reported the theoretical and experimental aspects of the electronic interactions between graphitic and Au NPs interface. The enhanced Raman signals obtained due to Surface-Enhanced Raman Scattering (SERS) on the graphitic interface with plasmonic nanoparticles. On the other hand, the mini Schottky barriers in nanoparticles decorated SWCNTs contribute to Field Effect Transducer (FET) as small changes in the electrical environment are also used to elucidate structures. The interaction of Au NPs with graphitic interface occurs through oxygen-containing defects.[138,139] The CNTs surface modified for nano assembly with metal nanoparticles *via* chemical oxidation, activation, and finally amidation reaction on the nanotube surface. Recently, Chinh *et al.*[140] reported the ox-MWCNT surface grafting with hydrosilane (HS) and finally achieved the covalent decoration of Au NPs on MWCNT. The systematic approach is shown in Fig. 4 which elaborates three steps process (i) functionalization of CNT surface using 3 : 1 H_2SO_4/HNO_3 (ii) zwitterionic thiolation reaction for grafting cysteaminium chloride, and (iii) covalent interaction of Au NPs with –SH group on CNTs surface. The authors took advantage of electrostatic interactions between negative MWCNT-COOH and positive primary amine groups of cysteamine and hence discarding any use of harmful chemicals[141]

Since the use of gas sensors limits due to considerable restrictions to their operation at optimum conditions. Majorly limitation is the reusability and responsiveness of sensor material. The better sensor must recover itself after analyzing gas molecules at an optimum temperature.[142] A higher temperature is generally applied for gas molecules' desorption on the sensor surface.[28,143] Sensors integrated on various solid surfaces for their better orientation, specific interactions, and uniform distribution of composite nanomaterials. Among different methods for incorporating gas sensors with CNTs, casting CNTs on IDEs is most common. Kumar *et al.* fabricated an interdigitated Au electrode coated with CNTs through a spin coating method.[144] The Au electrodes were fabricated on an insulating SiO_2 substrate by direct current sputtering in a chamber and spin coating of CNTs in a 1 M solution of isopropyl alcohol.

5.1.3 Gas sensing with Au NPs adsorbed on CNT surface. The gas sensors found useful environmental monitoring applications where contamination of food, toxic gas leaking, and chemical manufacturing industries. This section discusses the preparation, fabrication, and mechanism of gas sensing with AuNPs-CNTs heterostructures. CNTs, because of their metallic or semiconductor nature, large surface area, hollow spaces, and tubular structures, have been used as suitable candidates for gas sensors. To enhance nanosensors' sensitivity and specificity based on CNTs, fabrication of their surface carried out with suitable nanomaterials. Sheng *et al.*[145]

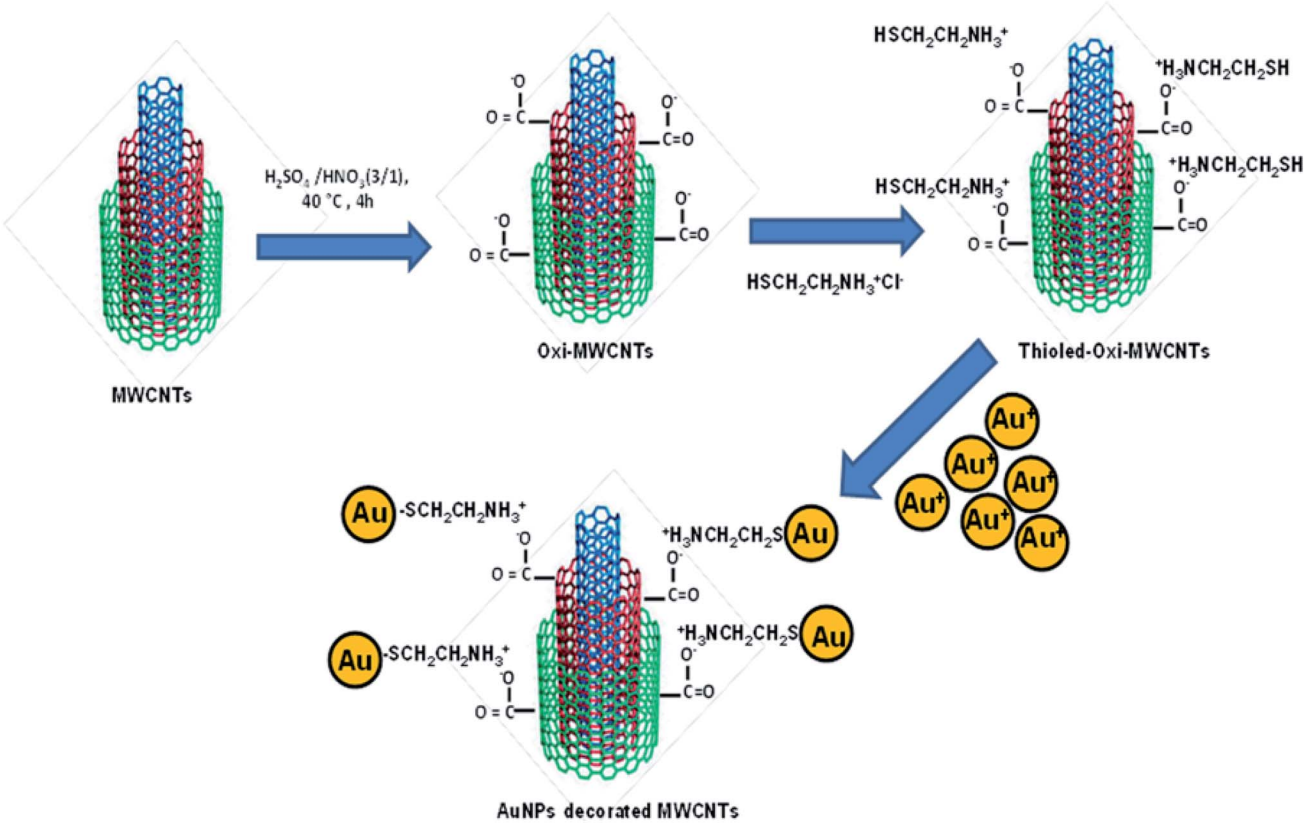

Fig. 4 Schematic illustration of covalent functionalization and decoration of Au NPs on ox-MWCNTs "this figure has been adapted/reproduced from ref. 140 with permission from Springer Nature, copyright 2019".

described Au NPs onto the surface of CNTs grown over Si substrate. The CNTs have grown on oxidized Si substrate with chemical vaporization deposition (CVD) method and an average 45 nm size of CNT obtained. The surface modification of CNTs with Au NPs shows enhanced sensitivity toward ethanol gas pumped with a maximum pressure of 800 mTorr. Since the p-type CNTs have grown on the Si substrate interact with reducing ethanol gas, it leads to an increase in resistance of CNTs. The different concentrations of vapors of ethanol gas were injected into the chamber, and the sensory response was recorded for bare CNTs and CNTs fabricated with Au NPs. It was found that sensor response increases for increased vapors concentration. Similar work was reported by Zheng-Dong Lin *et al.*[146] using the thermal CVD method for growing CNTs on the solid Si substrate at an elevated temperature around 700 °C. The sensor was successfully applied to detect CO_2 gas molecules up to 800 ppm level at room temperature. Authors also present Au NPs on CNTs grown on oxidized Si substrate and later converted on to a flexible polyimide substrate. The flexible and mobile nanosensors are currently in higher demand because of their broad applicability and low power consumption.[70] Kangho *et al.*[147] used polyethylene terephthalate (PET) as a flexible and transparent substrate for growing SWCNTs decorated with Au NPs for sensing NH_3 gas. SWCNTs spray-coated onto PET substrate and further Au NPs decorated on SWCNTs with electron beam evaporation technique.

Miniaturization of sensing materials and their fabrication interestingly enhances practicability. Microfabrication of sensing devices generally upholds various advantages over traditional techniques. Microfabrication platforms for sensing materials provide more comprehensive applications in wearables and the internet of things. Microelectromechanical system (MEMS) techniques are widely used to fabricate gas sensing devices.[148,149] Many literature reports based on MEMS fabricated gas sensors using Au-based materials have been published[150–152] in recent years. MEMS technology also offers a single miniaturized system to complex multifunctional systems. Some authors recently presented Au fabrication with Co_3O_4 nanoparticles and SnO_2 : NiO thin films on MEMS platform for NO_2 gas sensing. CNTs based gas sensors using MEMS platforms are also extensively developed in the past decade.[153–155] There are significant advantages of microsensor arrays based on MEMS technology, which include easy fabrication process, feasible industrial production, and enhanced stability/response of the sensor. However, there are very few reports on Au-CNTs based hybrid functionalized materials on the MEMS platform. Sharma *et al.*[156] demonstrated the MEMS technology for sensitive detection of H_2 gas. A thin film of Au/CNT composite material was fabricated on a substrate by direct current sputtering technique followed by dealloying process to obtain a regular sponge type structure with uniform and open porosities. The porous structure of the sensing array is

desirable for the increased surface area and enhanced mechanical strength. MEMS-based microsensor represents high sensitivity toward low concentration (below 100 ppm) of H_2 gas. In another study, Penza *et al.*[157] demonstrated CNTs network growth on alumina substrate with radio frequency plasma-enhanced CVD method (RF-PECVD). Both authors used acetylene as a carbon precursor for the growth of CNTs. The modification of CNTs surface with AuNPs achieved by rf magnetron sputtering and controlled thickness of 2.5, 5, and 10 nm obtained. NO_2 a known air pollutant detected by Au NPs-CNTs chemiresistor up to 200 ppb level at an operating temperature of 200 °C. The controlled loading of Au NPs on CNT affects the sensitivity and selectivity toward different gas molecules. In this context, Dilonardo *et al.*[158] reported controlled loading of Au NPs on MWCNT through electrophoresis and observed the impact of low and high Au loading on detecting gases. Authors found Au's high loading leads to preferential detection of H_2S while low loading of Au detects NO_2 gas. The plasma-enhanced CVD method produces randomly aligned CNTs for enhanced gas sensing application. However, the length of CNTs and vertical alignment of CNTs are more useful because of unidirectional electrical charge transport. Mudimela *et al.*[159] reported vertically aligned CNTs (VA-CNTs) grown over Si wafers. The Al_2O_3 (30 nm) and Fe (5 nm) layers deposited over native SiO_2 used been develop to form a multilayer (Si/native SiO_2/Al_2O_3/Fe) catalyst. Au NPs decorated over surface with physical vapor deposition technique (PVD). The length of CNTs used in the sensor plays a crucial role in sensing NO_2 gas.

Furthermore, they tested three types of lengths, 150 μm, 300 μm, and 500 μm, out of which 300 μm CNTs show optimum sensitive response toward NO_2. The increase in humidity from dry to 50% also increases the sensing response regardless of nanotubes' length. The vertical alignment and growth of the CNTs depend upon synthesis time and are explained with scanning electron microscopy (SEM). The estimated growth rate in CVD condition was 17.5 μm min^{-1}. The high-resolution TEM imaging represents the internally aligned MWNTs with defects on their surface. These graphitic defects on the surface are generally imperfections like breaks, dangling bonds, *etc.*, resulting from the tubes' low crystalline behavior. The magnetic sputtering of Au NPs on the CNTs surface leads to the random distribution of nanoparticles on the surface and spherical shape and mean diameter calculated around 6 nm (Fig. 5).

The sensing application of VA-CNT decorated Au NPs for NO_2 detection shows a decrease in resistance, concluding the VA-CNT carpet's p-type semiconducting behavior. The low-temperature growth of CNT affects the formation of defects on the surface. However, nanoparticle growth due to magnetic sputtering functionalized on top of the forest surface and did not follow the entire length of CNTs. Au–Au's binding energy is more than Au-CNT; hence, cluster formation of Au NPs at the surface is energetically favored than Au-CNT assembly. The defects that appear on the surface of CNTs significantly increases the binding energy between Au-CNT.[139] Charlier *et al.*[139] demonstrated CNT surfaces' functionalization by treating oxygen plasma to create structural and chemical defects. The defects further facilitate the fabrication of Au NPs. The procedure was carried out using inductively coupled plasma at RF frequency of 13.65 MHz, pressure 0.1 Torr, power 15 W for the one-minute duration. The authors also compared the sensing results with Au NPs adsorbed on a pristine CNT surface. The concluded remarks from TEM analysis show a better response and more uniform distribution of nanoparticles attributed to defects created by oxygen plasma treatment. The perfectly nucleating Au NPs at defective sites agreed with theoretical studies. The nanohybrid system shows a remarkable change in conductance values at the stipulated temperature range (25–150 °C) for NO_2 exposure at ppb level.

Jaewook *et al.*[160] demonstrated the binary type of NP-CNT composite for humidity sensors using a simple physiochemical method. In a two-step process, firstly positive charge bearing Au particles stacked on the surface of CNT and then gallic acid-modified iron oxide NPs (GA-IONPs) which act as reducing agent to synthesize Au NPs and while mixing with CNT-Au^{3+} solution both metal nanoparticles attach on CNT surface through pi–pi interactions (IA-CNT). The resulted IA-CNT composite aligned on Pt electrode placed on to magnetic

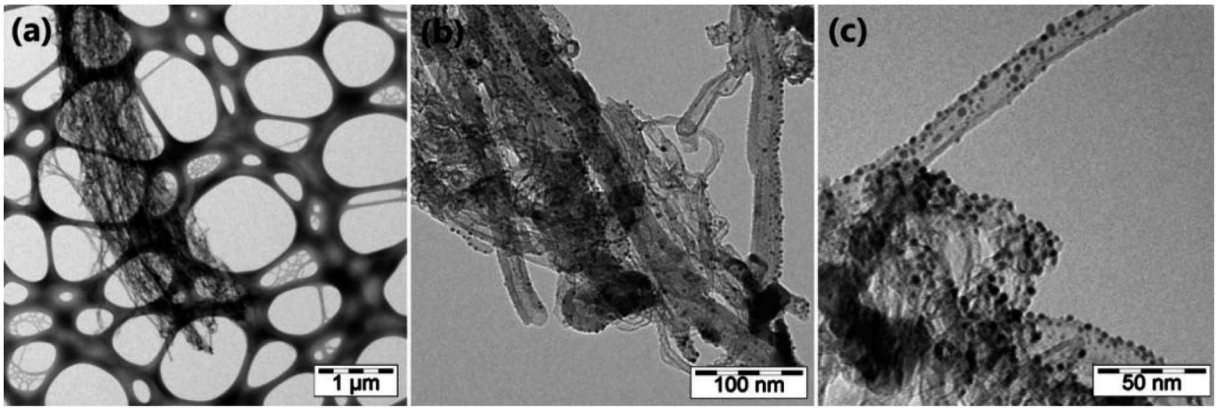

Fig. 5 TEM illustration of VA-CNT functionalized Au NPs "this figure has been adapted/reproduced from ref. 159 with permission from Beilstein Institute for the Advancement of Chemical Sciences, copyright 2014".

bars to get desired electrical properties. The straight and cross-alignment achieved by dispersing the solution of IA-CNT on Si wafers. The SEM analysis of aligned IA-CNT (shown in Fig. 6) obtained with magnetic force and surface tension of evaporated water. The parallel aligned IA-CNTs used as sensing channels on Pt electrode and show the linear response for relative humidity (RH) of 10%, 45%, and 70%. The water molecule adsorbed on the IA-CNT channel's surface creates a potential difference and increases the resistance. This increase in resistance is directly proportional to humidity. Authors also represent insignificant change sensitivity toward various gases such as dry air, CO, CO_2, SO_2, H_2, O_2, *etc.*, which accounts for the sensor's selectivity toward humid gas sensing.

In the progress of developing functionalized CNTs for enhanced selectivity and sensitivity toward different gases. Thamri *et al.*[161] reported functionalization of MWCNTs decorated Au NPs with a self-assembled monolayer of sixteen mercaptohexadecanoic acids (MHDA). The self-assembled monolayer (SAM) technique advantageously links CNT's outer surface with the thiol group present in MHDA. Before implying the SAM technique for functionalization, MWCNTs were treated with low oxygen plasma for creating oxygenated defects on their surface. Inductively-coupled plasma at RF-frequency 13.56 MHz created oxygen functionalities such as carbonyl, carboxyl, and hydroxyl on the CNT surface (Fig. 7). Thin films of plasma-treated MWCNTs were created on alumina substrate through airbrushing, and finally, Au NPs decoration was carried out through the sputtering method. A typical MHDA functionalization procedure on the nanoparticle surface through the SAM technique involves a long alkyl-thiol chain functionalized on the metal surface.[162] Functionalization includes 0.1 mM solution of MHDA in ethanol deposited on MWCNT-Au substrate kept at 4 °C and washed several times with ethanol followed by drying under N_2 flow. The prepared MWCNT-Au and MWCNT-Au-MHDA substrate tested for detection of aromatic (toluene, benzene), non-aromatic (ethanol, methanol, and acetone), and SARIN warfare agent dimethyl-methyl-phosphonate (DMMP). The MHDA functionalization affects the sensing behavior toward different analytes. The MWCNT-Au sensor exhibits response toward non-aromatic and aromatic volatile organic compounds (VOCs) while MWCNT-Au-MHDA does not show response toward aromatic VOCs. However, remarkable sensitivity toward non-aromatic VOCs and reversibility at room temperature recorded in case of MWCNT-Au-MHDA.

The different responsiveness of functionalized MWCNT-Au-MHDA was explained based on interactions with VOCs. Since π–π interactions are considerably responsible for aromatic VOCs to interact with the surface of CNT or Au NPs, which is prevented due to carboxylic group of MHDA results in the separation of aromatic VOCs from CNT surface.[163] Contrary, a reversible sensitive response toward non-aromatic VOCs was explained based on long-chain mercaptans' solubility in ethanol and acetone, which establishes the strong bonding between MHDA and non-aromatic VOCs. The hydrophilic groups like carboxyl enhance alcohol sensitivity and are responsible for sensitivity toward non-aromatic VOCs.[164] The Au NPs fabrication also significantly alters the sensing characteristics of composite materials. The even distribution and density

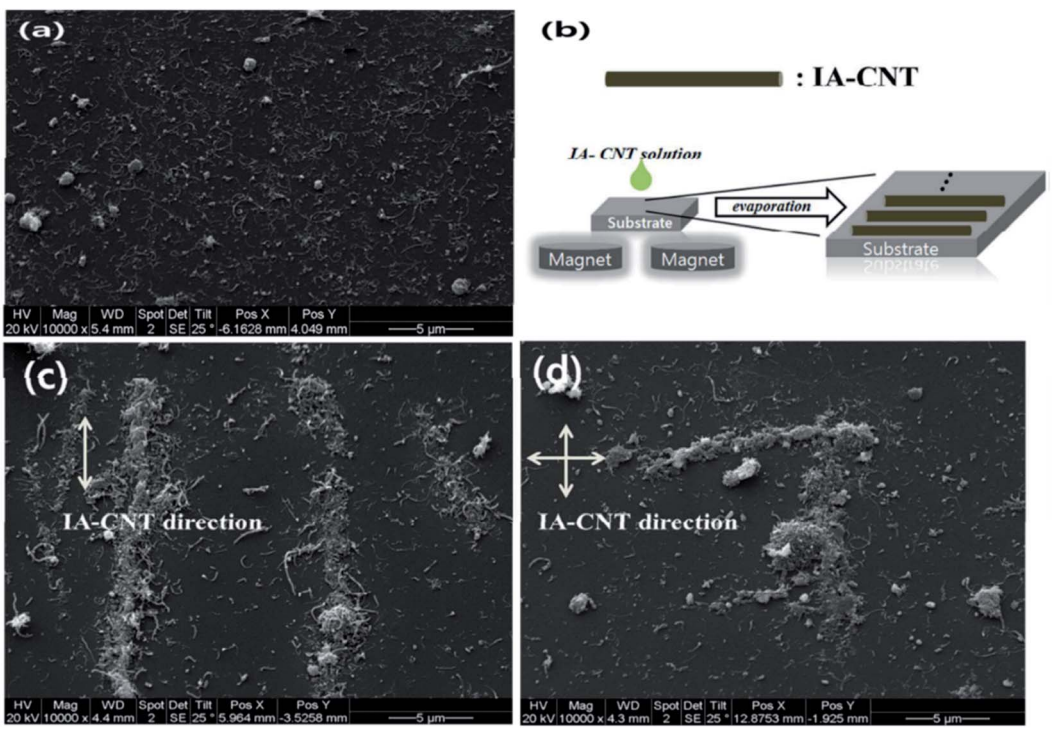

Fig. 6 (a) Pre-aligned IA-CNT SEM images, (b) alignment process, (c & d) parallel aligned and cross-aligned IA-CNT SEM images, respectively "this figure has been adapted/reproduced from ref. 160 with permission from American Chemical Society, copyright 2015".

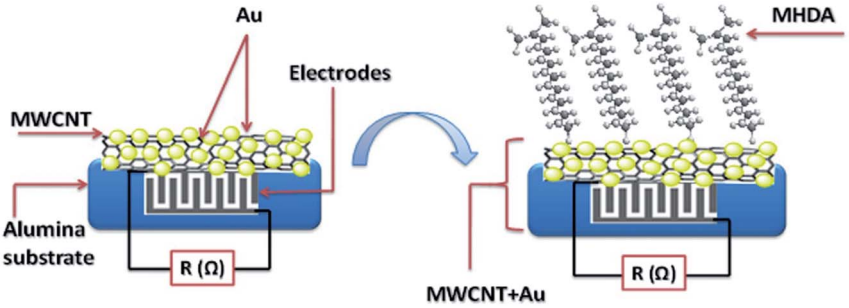

Fig. 7 Synoptic sensor structure based on MHDA deposited on carbon nanotubes decorated with gold nanoparticles "this figure has been adapted/reproduced from ref. 161 with permission from Springer Nature, copyright 2016".

of functionalized nanoparticles on the CNT surface enhance certain gases' sensing ability. The Brust method[165] explains the formation of thiol-capped Au NPs *via* a two-phase reduction procedure.

Further decoration of these capped Au NPs on acetone treated oxygenated defect containing CNT surfaces carried out by simple ultra-sonication.[166] The sensor designed for ultra-low sensing of NH_3 consists of two interdigitated electrodes (IDEs 5 × 5 mm) of copper on a plastic substrate (inter finger spacing 50 μm). Drop-casting 1 μL homogeneous dispersion of AuNPs/MWCNTs composite onto IDE is followed by vacuum annealing for two h at 100 °C in the oven.

In other studies, the oxygenated defects containing nanotubes (O-MWCNTs) were fabricated with Au NPs, and further functionalization was carried out with quinoxaline-walled thioether-legged cavitand 4 (cav-Au-MWCNT) for highly sensitive molecular recognition of benzene vapors.[167] The resistive sensor consists of two parts recognition and transducer elements embedded in an electronic device. Quinoxaline-bridged cavitand 4 includes one BTEX molecule having cavity size 8.3 Å, leading to a 1 : 1 host–guest complex. The fabrication of oxygen plasma-treated MWCNT resulted in defects that are proved with DFT studies. The DFT analysis also concludes that the Fermi energy level of MWCNT was a little shifted toward low energy in combination with Au NPs. This phenomenon is treated as a p-doping of nanotubes, where small charge transfer occurs from tube to Au NPs.[168] The cav-Au-MWCNT composite material has been used for resistive response and recovery under the increasing concentration of benzene vapors in dry air. The sensor reported described reversible and highly responsive for 100 ppb concentration of benzene than toluene or *o*-xylene. The sensitivity toward benzene is explained based on reversible host–guest interaction of benzene with cavitand 4. The cavitand 4 initially occupied with N_2 molecule from the air and show greater affinity for benzene than N_2 because of π–π and CH_2–π interactions. The stability of inclusion complex on CNTs surface modified with cavitand explained based on the vase and kite conformation followed by transduction mechanism of electron transfer. The kite conformation of N_2 captured cav-Au-MWCNT easily gets converted to vase conformation due to low energy barrier, and a new host-guest inclusion complex formed.[169] The benzene included cav-Au-MWCNT also possesses the two conformations on the surface having π–π stacking interactions. The stream of air modifies the equilibrium, and the catalyst recovers to its original state. The authors also emphasized the conformational exchanges on the surface lead to selective detection and recovery of the sensor.

Recently a group of researchers achieved fabrication of a one-dimensional Au NPs linear array with structural rigidity on protein-sheathed SWCNTs.[136] In a typical procedure, SWCNTs are sonicated in the presence of bovine serum albumin (BSA) protein leading to BSA-sheathed SWCNTs formation followed by deposition of Au NPs linear arrays through Au-thiol bonding with BSA. The 1D Au NPs array is further deposited with Ag and Pd/Ag metals to form nanowire structures similar to SWCNTs in the form of coalesced core–shell nanoparticle assembly.

The replication of SWCNTs with a super structured metal array exhibits great potential in sensing technologies. Another group reported a bottom-up approach to synthesize 1D Au nanowires (Au NWs) from self-assembly of Au NPs on CNTs followed by a thermal-induced nano-welding process. The process involves functionalizing CNTs with 1-pyrenesulfonic acid (PSA) to get the homogeneous suspension followed by dissolution and reduction of $HAuCl_4$ with sodium citrate at controlled 100 °C temperature.[170] TEM analysis indicates the assembly of Au NPs in the early stages, while later on, the fusion of NPs started at the reaction temperature. The interconnection between the NPs induced through the thermal heating process ultimately led to Au NWs after 120 minutes (Fig. 8). Longer heating time is required for the establishment of the interconnection and welding process.[171] The optical studies also present purple color's appearance due to redshift and conversion of Au NPs to Au NWs. The high-resolution TEM image in Fig. 8(A) signifies that the AuNWs possess a face-centered cubic structure.

There was no observable effect of SWCNTs on the fusion process and regarded as thermally induced welding of NPs to form Au NWs. The authors also provide theoretical studies for understanding the mechanism of self-assembly and thermal nano welding processes with different templates. Adsorption of citrate and PSA simulated theoretically on the Au_{20} cluster model and extended Au (111) surfaces. It has been concluded that the Au NPs functionalized with citrate adsorbed on the

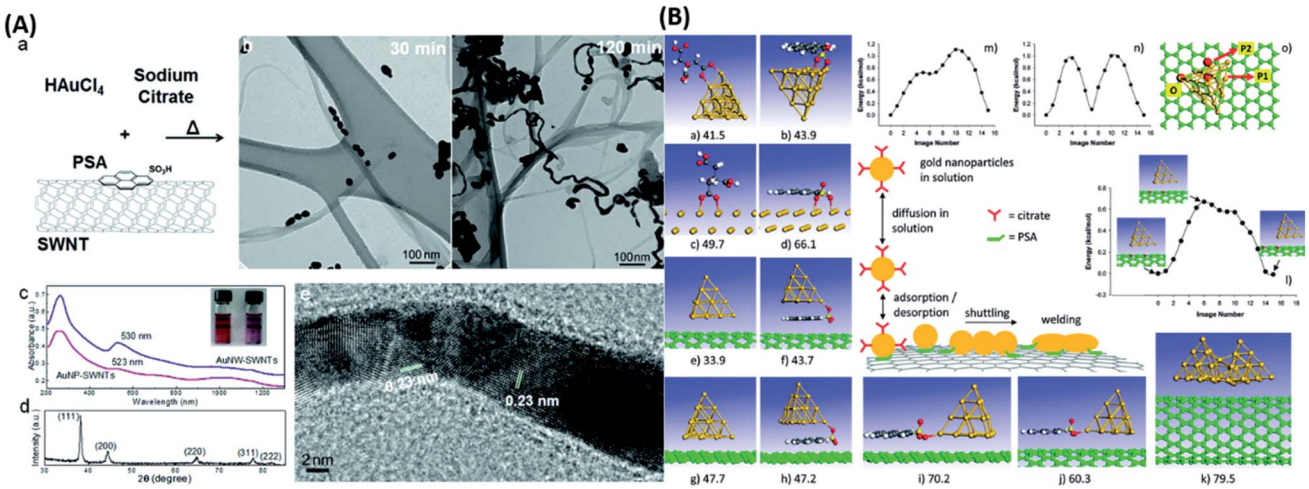

Fig. 8 (A) Synthesis process details representing (a) PSA-functionalized SWCNTs were used as a template during citrate reduction of $HAuCl_4$. (b) TEM images showing the assembly of AuNPs on the SWCNTs (after 30 min, left) and their welding into AuNWs (after 120 min, right). (c) UV-vis-NIR absorption spectra of AuNW-SWCNTs and AuNP-SWCNTs samples. The inset represents a digital photo of vials containing suspensions of AuNPs and AuNWs (with SWCNTs). (d) X-ray diffraction pattern of AuNWs. (e) High-resolution TEM image of AuNWs showing the polycrystalline nature of the welded AuNWs. (B) Detailed computational findings presenting molecular modeling, assembly, and nano welding processes "this figure has been adapted/reproduced from ref. 170 with permission from American Chemical Society, copyright 2012".

graphitic surface and through nano welding process 1D NWs or 2D-islands formed on SWCNTs surface. Theoretical studies also find a stronger interaction between PSA and Au NPs compared to citrate because of additional long-range interactions between the Au surface and aromatic carbon atoms. The Au_{20} cluster's adsorption on to graphitic surface also leads to binding interactions with PSA molecules through dispersion interactions and SO–Au bonds. Simulation of other graphitic templates for adsorption configuration carried out to comparative analysis. The detailed computational findings are presented in Fig. 8(B), which shows molecular modeling of the adsorption, assembly, and nano welding processes.

The middle panel represents a schematic description of the adsorption, diffusion, and mechanistic welding steps involved in forming Au NWs from Au clusters on CNT (graphene) surfaces decorated with PSA molecules. The indicated panels correspond as follows: adsorption configurations of citrate and PSA systems on an Au_{20} cluster (a and b) and Au (111) surface (c and d), respectively; adsorption configurations of an Au_{20} cluster on a bare and PSA decorated CNT (e, f and j) and on bare and PSA decorated graphene (g, h and i); and the welding of two Au_{20} clusters on CNT surface (k). Panel (l) represents the minimum energy pathway for diffusing an Au_{20} cluster on a CNT surface in an axial direction between two surface sites marked in red. Panels (m) and (n) represent the minimum energy diffusion pathways of the Au_{20} cluster on graphene surface starting from an initial position O and taken along two different directions *P*1 and *P*2, indicated by red arrows in panel (o). The indicated atomistic configurations correspond to the most stable states identified based on dispersion corrected DFT calculations. In each case, the corresponding binding energies (in kcal mol^{-1}) are given concerning the isolated adsorbate and surface subsystems. In panels (a–d), the adsorption energies of citrate and PSA ions are indicated, while in panels (e–k), the adsorption energies of the Au_{20} cluster are shown. For PSA and citrate systems, the C atoms are represented in gray, O atoms in red, H atom in white, and S atom in yellow; for graphene and CNT surfaces, the C atoms are shown in green, while the Au atoms are represented in orange.

New techniques for deposition of composite materials and fabrication of gas sensors include laser-induced forward transfer (LIFT). Generally, a small amount of donor material is deposited on the acceptor substrate without solvent and free from post-annealing procedures. The technique used for depositing nanoparticle thin films; however, Lasserre *et al.*[172] reported the LIFT technique for deposition of MWNTs decorated with Au/Pd NPs gas sensing array using femtosecond laser pulses. An ultrashort pulsed laser (1 kHz) with wavelength 800 nm used for the experiments, and by altering the number of pulses diameter of a nanoparticle can be adjusted.

5.1.4 Gas sensors based on CNTs grafted over Au NPs. Optical gas sensing properties have attracted significant attention by introducing metal nanoparticles to the sensor's arrays. As it is well known, Au NPs are associated with localized surface plasmon resonance (LSPR) effect.[173] LSPR changes the dielectric properties of associated species, and this characteristic is exploited for fabricating sensor devices. The interaction of Au NPs with CNTs apparently weak and generally defected areas targeted for bonding originated from the oxidation of pristine SWCNTs.[174] Alessandro Martucci *et al.*[175] developed a plasmonic-based gas sensor to detect hydrogen gas by designing transparent CNT optical film coupled with Au NPs. The Au monolayer deposited by spin coating technique at 3000 rpm for the 30 s over fused silica quartz functionalized with (3-aminopropyl) trimethoxysilane (APTMS). The Au monolayer substrate first functionalized with poly-L-lysine for deposition of SWCNTs.

The drop-casting method for sedimentation of SWCNT on the plasmonic surface suggested by the authors followed a simple procedure, and the desired deposition achieved in 3–20 h. However, they reported the inkjet printing method for their sensor demonstration because films deposited *via* drop-casting techniques show lesser optical responses than inkjet films.[176] The optical absorbance change in LSPR spectra is confined toward sensing of H_2 gas. Authors demonstrated both m-SWCNT and s-SWCNT toward gas sensing and concluded with the more efficient optical response with m-SWCNT because of better ohmic contact between Au NPs and SWCNTs. Table 1 summarises various gas sensors based on the assembly of CNTs and Au NPs, and analyte gases.

5.1.5 The mechanistic approach toward gas sensing using AuNPs/CNTs assembly. The semiconductor CNTs based sensors generally show mechanism according to electron transfer between gas molecules adsorbed on their surface. The type of mechanism is decided based on the nature of gas molecules, reducing or oxidizing. The oxidizing gas molecules (NO_2) adsorbed on CNTs surface lead to a decrease in resistance of CNTs and, on the other hand, reducing gas molecules (NH_3, CO, H_2S, N_2O) adsorbed on CNTs surface increases electric strength, categorized under the p-type mechanism. Bakhoum *et al.*[180] reported the resistance change during the detection of CO gas molecules on Au decorated CNTs. Au NPs have an affinity toward oxygen molecules, whereas, CO being reducing in nature, can combine with molecular or atomic oxygen and releases an electron. The extra electron decreases the overall resistance of the CNTs array. Sensor fabrication is equally vital in deciding the mechanism of gas adsorption and its sensing at desired levels. Kamarchuk *et al.*[192] demonstrated the Au microwires and SWCNTs point hetero contact (PHC) for sensing NH_3 and NO_2 gas vapors. The SWCNTs thin film deposited on to perfluorinated flexible polymer Nafion. The sensor's response was independent of Nafion polymer, and the electrical resistance properties of PHCs do not influence the Schottky barrier. Fig. 9 shows an increase in the PHC resistance for a single SWCNTs film and two Au-SWCNTs hetero contacts on short exposure (8 s pulse) to 1% NH_3. The rise in resistance was observed to be 100–150% from the initial value and exhibit remarkable relaxation time (200 s) compared to conventional SWCNTs. The PHC's extraordinary properties are explained by forming long channels between Au wires and SWCNTs surface where the diameter of channels was in nanometre or angstrom. The authors also describe the displacement technique to increase the number of point contact and consequently enhance the surface-to-volume ratio.[193]

Optical absorbance studies show that electronic transitions in SWCNTs give three absorbance bands in semiconducting SWCNTs while on the band in the case of metallic SWCNTs. The S_{11} band in semiconducting SWCNTs alters with electrons' addition, while the M_{11} band in metallic SWCNTs remains unaffected with the same.[194,195] The change in absorbance of the S_{11} band has been taken as a basis for any chemical interaction on the surface of semiconducting SWCNTs. A combination of theoretical studies with experimental data helps understand the NP-CNT electronic transfer when gas molecules are adsorbed onto them. Kauffman *et al.*[196] presented CO gas adsorption mechanism at room temperature on to AuNP-SWCNTs based on the combined electrical response, optical absorbance, and electronic structure calculations. Fig. 10 a compares UV-vis-NIR absorption peak of AuNP-SWCNTs in flowing N_2 and after 30 minutes exposure to 2500 ppm of CO at room temperature. The change in absorbance and slight blue shift attributed to transfer of electron to Au surface from 5σ orbital of adsorbed CO.

The S_{11} absorbance band and decrease in conductance also follow Langmuir-type-curves followed by electron transfer to SWCNTs. Density functional theory (DFT) studies indicate a strong correlation with experimental data and show CO's adsorption on the Au NPs surface. The DFT calculations were carried out on a single (14,0) SWCNTs decorated with an Au_{20} cluster. The energetically most favored adsorption site at Au_{20} corner with energy 20.1 kcal mol^{-1}. Fig. 10 mentions the adsorption of a higher number of CO molecules on Au NPs cluster decreases the conductance of Au-SWCNTs. The authors also explained the longer time scale response of Au NPs SPR than the response of semiconducting SWCNTs S_{11} absorbance and conductance-based on the increased interfacial potential barrier of Au-SWCNTs upon CO adsorption.[197] Another factor is Au NPs having a greater diameter than the electron mean free path (~50 nm), which restricts the transfer of electrons to SWCNTs through a potential interfacial barrier, consequently increasing the localized electronic environment Au NPs and promote SPR signal.[198,199]

NH_3 exposure to MWCNTs results in a decrease in CNTs channels' conductance due to an electron transfer from NH_3. The valence band shifted away from the Fermi level, which results in hole depletion, subsequently increasing resistance.[200] Hasnahena *et al.*[166] proposed a simple mechanism for NH_3 sensing using thiol capped Au NPs decorated on MWCNTs based on experimental findings. Au(0) state attached on the surface of MWCNT first interact with NH_3 on exposure, and there is a transfer of charge to metal, consequently increasing charge density into the 1D channel of MWCNTs. The authors explained the room temperature gas sensing procedures and the sensor's recovery at ambient conditions without purging into dry N_2. In a recent report on NH_3 sensing using SWCNTs, decorated Au NPs show electron transfer to the SWCNT network, complemented by Au NPs. The results obtained with decorated SWCNT compared with pristine SWCNTs show remarkable differences. The difference arises due to Au NPs, which provide better attachment for selective transfer of electrons between the adsorbed gas molecule and SWCNT surface.[177]

The work function of Au NPs and SWCNTs (5.0 and 4.7–4.9 eV respectively)[201,202] results in the transfer of electrons from SWCNTs to Au NPs at their interface and creates a Schottky type barrier.[203] However, this barrier is low as the difference in work function of these two is not significantly high. The flow of electrons between two is easy under the atmosphere of gases to be sensed. Choi *et al.*[183] demonstrated the expansion of conduction channels formed between Au NPs and SWCNT when oxygen species like O^-, O_2^-, and O^{2-} adsorbed on the surface. When reducing gas as CO is analyzed with composite

Table 1 Gas sensor based on the assembly of Au NPs and CNTs, fabrication methods, analyzing approaches, and analyte gases

Type of AuNP/CNT assembly	Method of sensor array preparation	Sensor type and operating temperature	Gases detected	Ref.
Tuned loaded AuNPs on CNTs grown over alumina substrate	RF-PECVD method	AuNP-CNTs chemiresistor based on resistance change/20–250 °C	NO_2, NH_3, CO, H_2S *etc*	157
SWCNTs/AuNPs grown over Si substrate	PECVD technique	Resistance change/40 °C	NH_3 gas/30 ppm	177
AuNPs adsorbed on CNTs sensing array	Thermal CVD method	Resistance change/room temperature	CO_2 gas	146
AuNPs@CNT on the flexible substrate	Thermal CVD method	Resistance change/room temperature	CO_2, NH_3, and isopropyl alcohol/800 ppm	178
AuNPs@CNTs on Si substrate	Thermal CVD method	Resistivity sensor/room temperature	Acetone vapour and NH_3 gas/800 ppm	179
Porous AuNPs/CNT on Si substrate	Direct current sputtering/MEMS technique	Resistivity sensor/325 °C	H_2 gas/1000 ppm	156
AuNPs adsorbed on CNT array	Electrodeposition method	Resistance change/room temperature	CO gas	180
AuNPs-SWCNTs-PET substrate	Electron beam evaporation method	Resistance change/room temperature	NH_3 gas/255 ppb	147
Metallic SWCNTs loaded on AuNPs film	Ink jet printing method	(LSPR) plasmonic optical response-based sensor/150 °C	H_2	175
AuNPs adsorbed on VA-CNTs	Thermal CVD method	Resistance change/150 °C	NO_2 gas	159
MWCNT/Au/MHDA	CVD and self-assembled monolayer technique	Resistance variation/room temperature	Aromatic, non-aromatic VOCs and dimethyl-methyl-phosphonate (DMMP)	161
CNTs/AuNPs on Si substrates	Thermal CVD method	Resistance/room temperature	Acetone vapours and NH_3 gas	179
Functionalized CNT sensing arrays with metal NPs	Chemical deposition/combination of five different sensor components	Chemo-resistive response and 2D principal component analysis (PCA)/room temperature	Multiple sensing applications in environmental monitoring, breathomics, and biomarker (NH_3, acetone, sodium hypochlorite, benzene, H_2S, NO_2, *etc.*)	181
AuNPs/PANI/MWCNT	Chemical adsorption and polymerization	Change in electrical conductance/ room temperature	NH_3 gas, 200 ppb to 10 ppm linear response	182
AuNPs-SWCNTs IDEs	Dipping, self-agglomeration, and thermal method	Resistance change/room temperature	CO, NH_3, C_3H_6O, C_7H_8, C_6H_6, and NO_2 at 2 ppm concentration.	183
AuNPs–NH_2–MWCNT IDEs	Electro spraying/photolithography technique	Conductance change/22 °C	Polar (H_2O, propanol, ethanol) and non-polar (hexane, toluene, chloroform, *etc.*) VOCs/100–5000 ppm	70
AuNPs/SWCNTs Au electrode	Electroplating technique	Resistance change/room temperature	Hg vapours/∼2 ppb	184
Graphene/AuNPs	CVD and photolithography	Resistance change/room temperature	NH_3 gas/58 ppm	185
rGO/TiO_2/AuNPs ternary composite	Electroplating/photolithography	Resistance change/room temperature	NH_3 gas/2 ppm	186
Au decorated rGO/ZnO	Pulsed intense UV ablation process	Resistance change/room temperature under UV irradiation	H_2 gas	187
B-rGO/Au@SnO_2 heterostructures	Radio frequency magnetron sputtering and annealing	Resistance change/100 °C	Tetraethylamine gas	188
AuNPs@NPC-rGO ternary composites	Pyrolysis/membrane electrode assembly	Electrocatalytic current measurments and electrochemical sensing.	Hydrogen gas	189
rGO@CGN (carbon Au nanocomposites) electrochemical gas sensor	Electrochemical reduction/screen printing	Chronoamperometry/double potential amperometry/room temperature	O_2 gas (0.42–21%)	190
Graphene nanoribbon/Au electrodes	Standard deposition/ photolithography	Resistivity change/room temperature	NH_3 gas/25 ppm	191

material, it shows enhanced variation in the conduction channel. The more significant increase in resistance than oxidizing gases and higher sensitivity of CO up to 2 ppm attributed to the electronic effects between Au NPs and CNT and catalytic properties of Au NPs. It has been proved that Au NPs act as catalyst for complete oxidation of CO adsorbed to them.[204]

The polar and non-polar VOCs interacted differently with Au NPs. Tasaltin *et al.*[70] explained the mechanism of Au NPs filtration layer for sensing response for polar molecules where

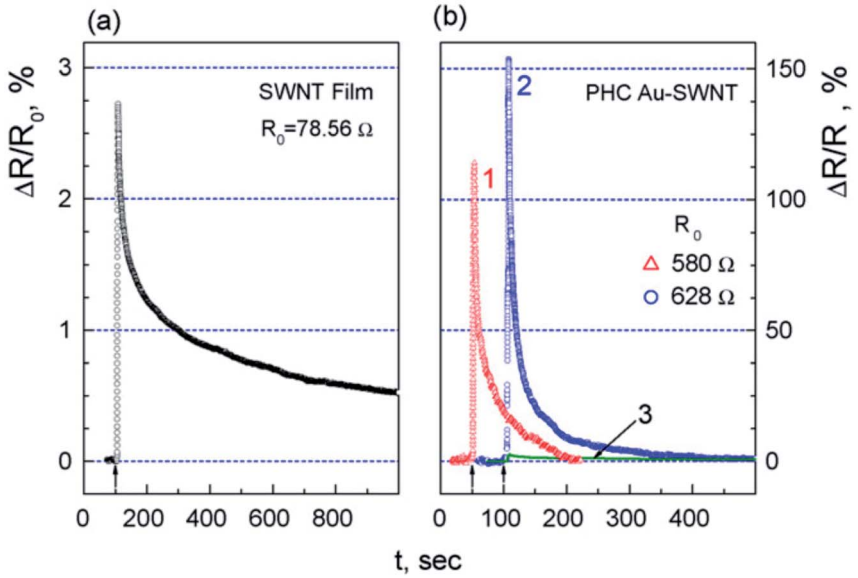

Fig. 9 Change of resistance for (a) SWCNTs film and (b) two Au-SWCNTs heterocontacts in response to 8 s pulse of one percent NH_3 (curves 1 and 2). For easy comparison with the point contact data on an equal scale, curve 3 represents the data in (a) "this figure has been adapted/reproduced from ref. 192 with permission from Elsevier, copyright 2008".

Au NPs interact with high polar molecules like water, ethanol, and propanol cannot reach up to conduction channel in MWCNT. The amine-functionalized nanotubes (NH_2-MWCNT) containing defects bind with adsorbed gas molecules effectively through electronic interactions. The Au NPs block the surface by interacting with polar analytes, but when authors increase the concentration of NH_2-MWCNTs and decrease Au NPs eventually increases the possibility of VOCs reaching defect sites.

Theoretical studies show coherence with experimental findings for sensing of gases through CNT modified with Au NPs. In

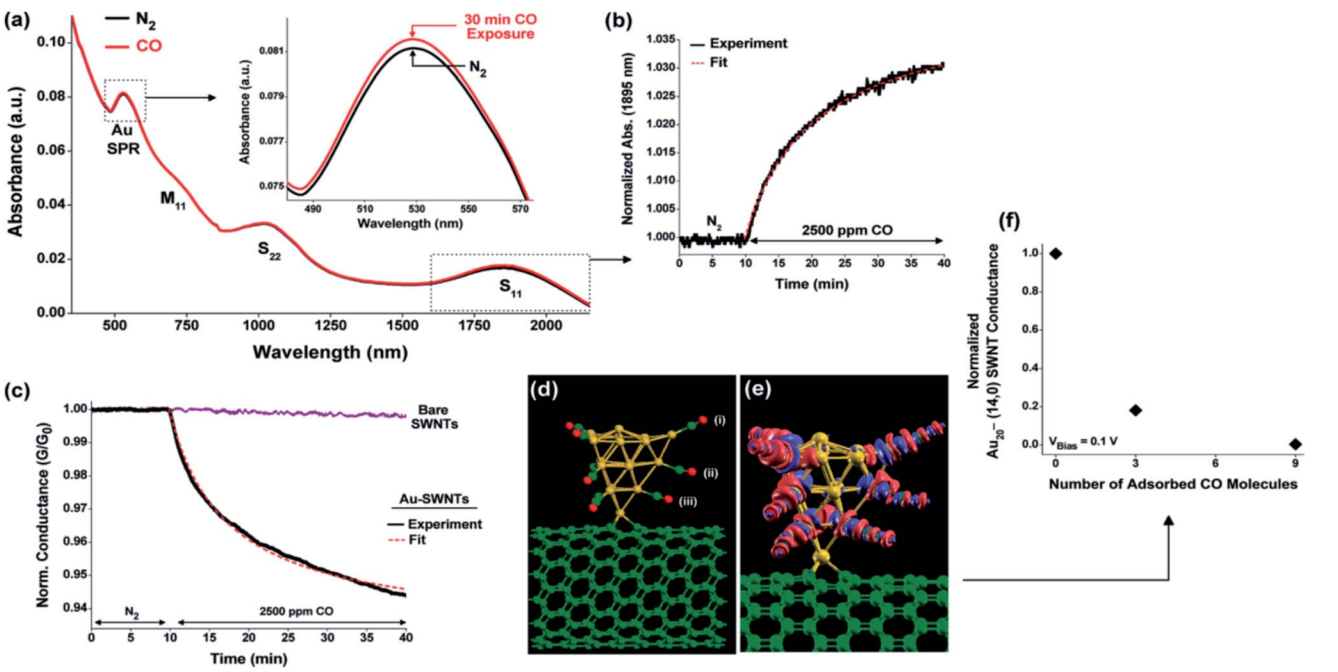

Fig. 10 (a) UV-vis-NIR absorption spectra of an Au-SWCNTs network under N_2 (black curve) (b) the absorbance of the Au-SWCNTs network S11 band at 1895 nm during CO exposure. (c) Normalized network conductance (G/G_0) of bare SWCNTs and Au-SWCNTs during exposure to CO gas. (d) Adsorption configuration and (e) charge variation map depicting nine CO molecules attached to the corner (i) and edge (ii and iii) sites of an Au_{20} cluster on a defective (14,0) SWCNTs; Au atoms are yellow, C atoms are green, and O atoms are red "this figure has been adapted/reproduced from ref. 196 with permission from American Chemical Society, copyright 2010".

such studies, Zanolli *et al.*[168] reported the (5,5) SWCNTs modified with 13-atoms Au nanocluster (Au_{13}) as a model system to detect gases like CO, NO_2, and C_6H_6. The model successfully explains the stronger interactions of NO_2 compared with C_6H_6 and also the decrease in resistance due to p-type doping. The Au_{13} is the most stable and relaxed SWCNTs-icosahedral Au_{13} system was chosen for studies because of total low energy (1.15 eV) and high binding energy (0.6 eV) than SWCNTs-cuboctahedral system. Fig. 11 explains the bonding of NO_2 through nitrogen because of polarity difference, and in the case of CO and C_6H_6, Au cluster bind through the carbon atom. The computed binding energy calculations show stronger bonding in the case of NO_2 while the least bonding in the case of C_6H_6. The lowest unoccupied molecular orbital (LUMO) of NO_2 lies below the Fermi energy level of the Au_{13}-SWCNTs system, hence, accepts significant electron density from both Au_{13} (0.289 e^-) and (5,5) SWCNTs (0.218 e^-). The p-type semiconducting character further lowers the Fermi energy level and subsequently decreases in resistance observed. However, the weak interaction of C_6H_6 with the Au cluster increases the Fermi energy level, as shown in Fig. 11.

McNicholas *et al.*[184] reported the ultra-low detection of Hg vapors with a sensor consisting of SWCNTs modified Au NPs through a simple resistance change mechanism. The SERS signals are produced in SWCNTs while coupling with Au NPs.[205] The detailed mechanism of SERS has also been confirmed by the authors using absorption parameters of Hg vapors on the nanoparticle surface. The mechanism of Hg absorption was studied in detail, and concluded that the resistance increased when absorption of vapor occurs, and this is attributed to the transfer of electrons to holes in SWCNTs. However, bare SWCNTs adsorbing Hg vapor do not show a significant change in resistance. Hence, Au NPs are crucial for adsorbing Hg vapors and the transfer of electrons from the nanoparticle to the SWCNTs surface, leading to a change in resistance value. The SERS mechanism can be due to electrons' transfer between Au NPs and SWCNTs or plasmon resonance between them.[206] The absorption of Hg on the nanoparticle surface should enhance SERS signals' intensity due to increased electron transfer. Still, the authors found no significant change in the signal indicating the plasmonic resonance coupling between Au NPs and SWCNTs.

5.2 Au NPs-graphene heterostructures for gas sensing

The fabrication of heterostructures based on Au NPs and graphene has been utilized for the sensing devices. GO layers are easily fabricated with AuNPs to perform plasmonic sensors or electrochemical sensors.[207,208] The detection of various toxic gases such as NH_3 and NO_2 using 2D graphene-based composites is highly desired, lacks selectivity, and has a tiny response. Hence, 2D composites were fabricated with AuNPs because of the previously described properties of these NPs to enhance the sensitivity of devices.

Furue *et al.*[209] reported a sensor for detecting inorganic arsine gas using rGO and thin Au films. The sensing ability of bare rGO and Au was not observed for this gas. The arsenic is a soft metal and hence expected to have an affinity with Au, consequently prompted authors to prepare interdigitated electrodes using rGO and Au. The Au/rGO device was fivefold less conductive than rGO, proving that Au does not increase the conductivity. The oxygen on Au islands replaced by the analyte gas and holes in Au increase the conductivity. For the fabrication of Au on the graphene surface, oxygen functionalities play an important role by providing reactive sites for nucleation and growth. Goncalves *et al.*[210] reported nanoparticles' development on the rGO surface in the aqueous medium. The growth was not observed on completely reduced surfaces, while growth was directly associated with the surface's degree of oxygen functionalization.

Gautam *et al.*[185] reported the sensing response of NH_3 gas at room temperature up to 58 ppm using graphene and AuNP composite sensor fabricated *via* CVD technique. They grow graphene sheets on Cu surface in an alumina tube furnace and further transfer them to suitable surfaces through itching and lift-off processes. Further, AuNPs are decorated onto the surface of graphene sheets through the reduction of $HAuCl_4 \cdot 3H_2O$. The energy band diagram of graphene metal contacts describes the sensing mechanism of heterostructures toward NH_3 gas. The

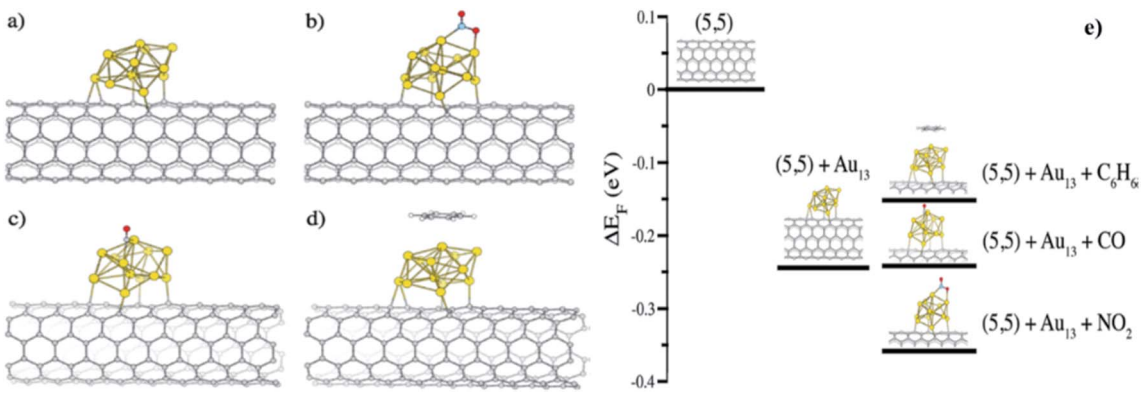

Fig. 11 Ball-and-stick models illustrating (a) (5,5) SWCNTs-Au_{13} nanocluster, interactions of adsorbed molecules (b) NO_2, (c) CO, (d) C_6H_6, and (e) theoretical shift of the Fermi energy (ΔE_F) of pristine (5,5) SWCNTs-Au_{13}, interaction with C_6H_6, CO, and NO_2 gas molecules "this figure has been adapted/reproduced from ref. 168 with permission from American Chemical Society, copyright 2011".

authors described the more p-type character of graphene due to the transfer of electrons from graphene to Au, which subsequently changes to less p-type when exposed to NH_3 due to dissociation of gas at Au surface.[211]

More recently, Zhou *et al.*[186] ternary composite of rGO, TiO_2 NPs, and AuNPs for NH_3 gas sensing at room temperature enhance UV illumination. The ternary composite acts as a chemiresistive sensor where graphene surface provides active sites for attachments of NPs and serves as a center for electron collectors and transporter. The Au NPs is to increase the sorption and enhance the charge separation of electron–hole pairs. The IDEs were fabricated using photolithography and lift-off methods. Fig. 12(a–d) shows the transmission electron microscopy of the ternary composite formed where it indicates the distribution of TiO_2 NPs on the basal plane of the rGO sheet. The TiO_2 NPs act as both NH_3 and UV-sensitive material. The Au NPs are directly associated with TiO_2 NPs and seldom with rGO sheets. Fig. 12(e and f) described the UV illumination role where the response toward 10 ppm NH_3 and a decrease in the baseline resistance observed on UV illumination indicate the sensing layer's n-type semiconducting properties. Fig. 12(e) clearly shows that the enhanced sensor response, better recovery time, and increased response speed compare with dark mode.

The author's probable mechanism for ternary composite material toward NH_3 sensing includes p–n heterojunctions of rGO/TiO_2/AuNPs sensor layers that withdraw electrons from NH_3 adsorption and result in an increase in the resistance. Lee *et al.*[212] demonstrated the defect-engineered graphene-based FET for enhanced sensing of NO_2 and NH_3. The defects were created intentionally on the surface by oxygen plasma and conventional reactive ion etching technique (RIE). The oxidation process in RIE leads to the reaction of oxygen radicals with carbon atoms on the surface of graphene, leading to sp^3 type defects. The defects increased the disorder due to the detachment of carbon in the form of CO and CO_2. FET structure is made up of a back-gate electrode by deposition of Ti/Au (20/80 nm). Fig. 12(g–k) shows the DFT studies indicating the strong adsorption of NH_3 on vacancy defect site in graphene. The adsorption energy of the NH_3 molecule increases with the formation of defects. However, the sensing response was also dependent upon the density of the defects.

More recently, Peng *et al.*[188] demonstrated the heterostructures of boron-doped rGO (B-rGO) coated with Au@SnO_2. The sensor was successfully applied to selectively sensing tetraethylamine gas up to ppb level at 100 °C. The metal oxide-based gas sensors are well known for their negative oxygen species attached to the surface, consequently reacting with analyte gas and decreasing the resistance. The two hetero-interface *viz* B-rGO and Au@SnO_2 play a crucial role in developing a potential barrier at the interface due to built-in potential. Hence when analyte gas interacts, there is a huge change in the resistance. However, boron doping in the rGO surface creates defects, leading to enhanced selectivity toward gas molecules.[213] Another report described the heteroatom doped rGO decorated with AuNPs for both liquid and gaseous phases of hydrazine detection.[189] The authors used N-doped porous carbon anchored on rGO nanosheets (AuNPs@NPC-rGO) in zeolite imidazolate framework-67 (ZIF-67). The synergistic effect of the ternary composite materials leads to a low detection limit of the sensor.

6. Summary and future perspectives

Experimental details showed the promising and conspicuous use of carbonaceous materials, mainly CNTs and graphene-based heterostructures with Au in the field of sensing technology. These materials' unique structure and supernal properties further make them special in sensing various gases and other volatile organics. The modification of surface properties with different organic or inorganic functionalities has been revamping the nanomaterial toward different applications. Surface modification of CNTs with functionalities enhances selective and specific results. The assembly of CNTs with metal nanoparticles proved its potential toward adsorption and electron transport channel for gas sensing. The assembly of CNTs with AuNPs produces different heterostructures, including 1D and 2D arrays, a bottom-up fabrication technique. The combined theoretical and experimental approaches also contribute to finding out the nature of Au nanocluster and interaction with the CNT surface. Theoretical simulations predict the binding energies and predict the intrinsic electronic properties and helpful in calculating electron transport. Tailored synthesis of CNTs using various methodologies and fabricating AuNPs to surface enhances selective response for different gas molecules. Chemiresistor gas sensors based on CNT and AuNPs array have potential toward different analytes; however, the gas sensor's recovery time plays a crucial role in real-time application. Research on these sensing probes has established various objectives such as fast recovery time, room temperature operational probes, highly sensitive and specific response, and sensor probes' cost-effectiveness. The investigations on the graphene and reduced graphene oxide-based heterostructures have shown exciting results for gas sensing due to exceptional mechanical, electrical, optical, and magnetic properties. The facile synthesis methods, easy availability of graphene precursors, and tunable properties can lead to the large-scale synthesis and construction of chemical sensors. The defect engineering in graphene and tuning its edges could further enhance the sensitivity and selectivity of chemical sensors.

It is noteworthy to mention here that, despite the extensive reports in Au–carbon-based materials heterostructures for gas sensing applications, many challenges need to be overcome with regard to the wide applicability of these materials' large-scale production. In this direction, these heterostructures' structural stability and surface modifications need to be improved by developing more facile synthesis techniques and more selective sensing applications. Moreover, the fabrication of nanospheres-based heterostructures results in excellent gas-sensing performance, but such materials' aggregation is one of the hurdles in integrating gas sensing devices. Furthermore, the synthesis of Au's 1D heterostructures with the uniform surface for facilitated charge transport is difficult to achieve. However, 2D materials-based heterostructures have shown promising

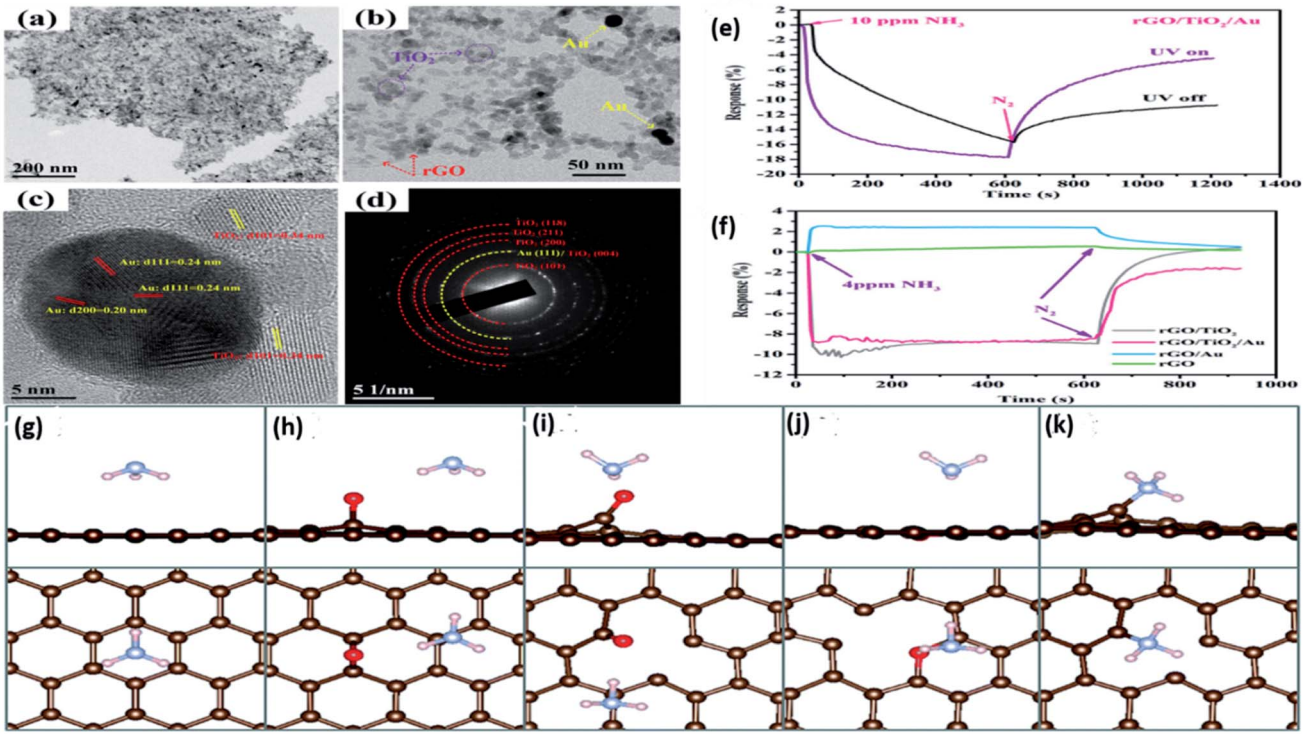

Fig. 12 (a–d) TEM images of ternary composites of rGo/TiO_2/AuNPs their local magnification, HRTEM image, and SAED patterns, (e) impact of UV on the composite sensory response, (f) ingredient combination response on the exposure of NH_3 gas when UV is on and off state "this figure has been adapted/reproduced from ref. 186 with permission from American Chemical Society, copyright 2018" (g–k) DFT analysis and optimized structures of NH_3 adsorbed on pristine graphene, sp^3 type defect epoxy group, carbonyl group, ether group-containing graphene, and single vacancy graphene, respectively. The first and second rows represent side and top views, while red, brown, grey, light pink colors represent O, C, N, and H atoms "this figure has been adapted/reproduced from ref. 212 with permission from Royal Society of Chemistry, copyright 2016".

results for gas sensing applications, but their large-scale production is still challenging. Therefore, more dedicated efforts are anticipated from the scientific community to explore the techniques which could pave the way towards a large-scale synthesis of these heterostructures.

Additionally, the selectivity and sensitivity of gas sensing devices could be sufficiently improved by fabricating 2D materials having excellent adsorption behavior, suitable interface construction, and controlled thickness of layered materials. A more detailed exploration of synthetic routes based on ideal reaction conditions for carbon-based heterostructures requires understanding the influence of heterointerface formation and sensing mechanism. The challenges like optimizing 2D materials and well-aligned hetero-interfaces with tunable properties must be considered during the fabrication process. In our understanding, the research in this field is still in the primary stage, and further systematic investigations, such as rational design and development of robust gas sensing devices with improved selectivity and sensitivity, are highly anticipated. In order to boost extensive research in this field, in addition to the 2D carbonaceous materials, the layered metal dichalcogenides, particularly MoS_2 and WS_2, have emerged as ideal materials for gas sensing applications. The heterostructures based on layered metal dichalcogenides with Au and other noble metals could result in the excellent sensing response for molecules such as NO_2, NH_3, H_2 *etc.* In addition to this, other layered 2D inorganic materials such as boron nitride (BN), MXenes, silicene, and germanene could be extensively explored for the fabrication of gas sensing devices. Furthermore, the design and development of heterostructures comprising of the 2D-3D assembly could open a new gate in the field of gas sensing.

Conflicts of interest

There are no conflicts to declare.

Acknowledgements

The authors are thankful to Deshbandhu College, University of Delhi, India, for providing research facilities.

References

1 S. Feng, *et al.*, Review on smart gas sensing technology, *Sensors*, 2019, **19**(17), 3760.
2 J. Bobin, J.-L. Starck and R. Ottensamer, Compressed sensing in astronomy, *IEEE Journal of Selected Topics in Signal Processing*, 2008, **2**(5), 718–726.
3 Y. S. Kim, *et al.*, Room-temperature semiconductor gas sensor based on nonstoichiometric tungsten oxide nanorod film, *Appl. Phys. Lett.*, 2005, **86**(21), 213105.

4 N. Golego, S. Studenikin and M. Cocivera, Sensor photoresponse of thin-film oxides of zinc and titanium to oxygen gas, *J. Electrochem. Soc.*, 2000, **147**(4), 1592–1594.
5 M. Aslam, *et al.*, A highly selective ammonia gas sensor using surface-ruthenated zinc oxide, *Sens. Actuators, A*, 1999, **75**(2), 162–167.
6 H. Bai and G. Shi, Gas sensors based on conducting polymers, *Sensors*, 2007, **7**(3), 267–307.
7 D. J. Wales, *et al.*, Gas sensing using porous materials for automotive applications, *Chem. Soc. Rev.*, 2015, **44**(13), 4290–4321.
8 X. Liu, *et al.*, A survey on gas sensing technology, *Sensors*, 2012, **12**(7), 9635–9665.
9 P. Kumari, *et al.*, Cyclodextrin-based nanostructured materials for sustainable water remediation applications, *Environ. Sci. Pollut. Res.*, 2020, **27**, 32432–32448.
10 S. Lal, A. Singhal and P. Kumari, Exploring carbonaceous nanomaterials for arsenic and chromium removal from wastewater, *J. Water Process.*, 2020, **36**, 101276.
11 S. Kumar, *et al.*, Visible light-assisted photodegradation by silver tungstate-modified magnetite nanocomposite material for enhanced mineralization of organic water contaminants, *Appl. Nanosci.*, 2020, **10**(5), 1555–1569.
12 S. Kumar, *et al.*, Recent Progresses in Organic-Inorganic Nano Technological Platforms for Cancer Therapeutics, *Curr. Med. Chem.*, 2020.
13 A. Singhal, P. Kumari and K. Nisa, Facile One-Pot Friedlander Synthesis of Functionalized Quinolines using Graphene Oxide Carbocatalyst, *Curr. Org. Synth.*, 2019, **16**(1), 154–159.
14 P. Kumari and H. Parashara, β-cyclodextrin modified magnetite nanoparticles for efficient removal of eosin and phloxine dyes from aqueous solution, *Mater. Today*, 2018, **5**(7), 15473–15480.
15 P. Kumari, *et al.*, Efficacious and selective oxidation of atrazine with hydrogen peroxide catalyzed by magnetite nanoparticles: influence of reaction media, *ChemistrySelect*, 2018, **3**(7), 2135–2139.
16 P. Kumari, *et al.*, Efficient reduction of C–N multiple bonds catalyzed by magnetically retrievable magnetite nanoparticles with sodium borohydride, *Catal. Lett.*, 2016, **146**(10), 2149–2156.
17 M. S. Mauter and M. Elimelech, Environmental applications of carbon-based nanomaterials, *Environ. Sci. Technol.*, 2008, **42**(16), 5843–5859.
18 M. M. Rana, *et al.*, A review on recent advances of CNTs as gas sensors, *Sens. Rev.*, 2017, **37**(2), 127–136.
19 W. Yang, *et al.*, Two-dimensional layered nanomaterials for gas-sensing applications, *Inorg. Chem. Front.*, 2016, **3**(4), 433–451.
20 J. Chen, *et al.*, Solution properties of single-walled carbon nanotubes, *Science*, 1998, **282**(5386), 95–98.
21 D. N. Futaba, *et al.*, Shape-engineerable and highly densely packed single-walled carbon nanotubes and their application as super-capacitor electrodes, *Nat. Mater.*, 2006, **5**(12), 987.
22 C. J. Lee, J. H. Park and J. Park, Synthesis of bamboo-shaped multiwalled carbon nanotubes using thermal chemical vapor deposition, *Chem. Phys. Lett.*, 2000, **323**(5–6), 560–565.
23 M. S. Dresselhaus and P. Avouris, Introduction to Carbon Materials Research, in *Carbon Nanotubes: Synthesis, Structure, Properties, and Applications*, ed. M. S. Dresselhaus, G. Dresselhaus, and P. Avouris, 2001, Springer Berlin Heidelberg, Berlin, Heidelberg, pp. 1–9.
24 G. E. Rakov, Methods for preparation of carbon nanotubes, *Russ. Chem. Rev.*, 2000, **69**(1), 35–52.
25 C. De las Casas and W. Li, A review of application of carbon nanotubes for lithium ion battery anode material, *J. Power Sources*, 2012, **208**, 74–85.
26 D. Vairavapandian, P. Vichchulada and M. D. Lay, Preparation and modification of carbon nanotubes: review of recent advances and applications in catalysis and sensing, *Anal. Chim. Acta*, 2008, **626**(2), 119–129.
27 N. Hiremath, J. Mays and G. Bhat, Recent developments in carbon fibers and carbon nanotube-based fibers: a review, *Polym. Rev.*, 2017, **57**(2), 339–368.
28 I. V. Zaporotskova, *et al.*, Carbon nanotubes: Sensor properties. A review, *Mod. Electron. Mater.*, 2016, **2**(4), 95–105.
29 T. Kavinkumar and S. Manivannan, Synthesis, Characterization and Gas Sensing Properties of Graphene Oxide-Multiwalled Carbon Nanotube Composite, *J. Mater. Sci. Technol.*, 2016, **32**(7), 626–632.
30 A. H. Castro Neto, *et al.*, The electronic properties of graphene, *Rev. Mod. Phys.*, 2009, **81**(1), 109–162.
31 K. Toda, R. Furue and S. Hayami, Recent progress in applications of graphene oxide for gas sensing: A review, *Anal. Chim. Acta*, 2015, **878**, 43–53.
32 A. Abdelhalim, *et al.*, Highly sensitive and selective carbon nanotube-based gas sensor arrays functionalized with different metallic nanoparticles, *Sens. Actuators, B*, 2015, **220**, 1288–1296.
33 Y. J. Kwon, *et al.*, Selective detection of low concentration toluene gas using Pt-decorated carbon nanotubes sensors, *Sens. Actuators, B*, 2016, **227**, 157–168.
34 M. Asad, *et al.*, High sensitive and selective flexible H2S gas sensors based on Cu nanoparticle decorated SWCNTs, *Sens. Actuators, B*, 2015, **210**, 1–8.
35 I. Uechi and S. Yamada, Photochemical and analytical applications of gold nanoparticles and nanorods utilizing surface plasmon resonance, *Anal. Bioanal. Chem.*, 2008, **391**(7), 2411–2421.
36 S. Guo and E. Wang, Synthesis and electrochemical applications of gold nanoparticles, *Anal. Chim. Acta*, 2007, **598**(2), 181–192.
37 C. Matricardi, *et al.*, Gold nanoparticle plasmonic superlattices as surface-enhanced Raman spectroscopy substrates, *ACS Nano*, 2018, **12**(8), 8531–8539.
38 S. Eustis and M. A. El-Sayed, Why gold nanoparticles are more precious than pretty gold: noble metal surface plasmon resonance and its enhancement of the radiative

and nonradiative properties of nanocrystals of different shapes, *Chem. Soc. Rev.*, 2006, **35**(3), 209–217.
39 N. Singh, R. K. Gupta and P. S. Lee, Gold-Nanoparticle-Functionalized In2O3 Nanowires as CO Gas Sensors with a Significant Enhancement in Response, *ACS Appl. Mater. Interfaces*, 2011, **3**(7), 2246–2252.
40 Z. Zhu, *et al.*, A Critical Review of Glucose Biosensors Based on Carbon Nanomaterials: Carbon Nanotubes and Graphene, *Sensors*, 2012, **12**(5), 5996–6022.
41 S. Yang, *et al.*, Advances in the use of carbonaceous materials for the electrochemical determination of persistent organic pollutants, *Microchim. Acta*, 2018, **185**(2), 1–14.
42 C. Cantalini, *et al.*, Carbon nanotubes as new materials for gas sensing applications, *J. Eur. Ceram. Soc.*, 2004, **24**(6), 1405–1408.
43 Y. Ando and S. Iijima, Preparation of carbon nanotubes by arc-discharge evaporation, *Jpn. J. Appl. Phys., Part 2*, 1993, **32**, L107.
44 A. Thess, *et al.*, Crystalline Ropes of Metallic Carbon Nanotubes, *Science*, 1996, **273**(5274), 483–487.
45 S. Arepalli, Laser ablation process for single-walled carbon nanotube production, *J. Nanosci. Nanotechnol.*, 2004, **4**(4), 317–325.
46 O. Jašek, *et al.*, Carbon nanotubes synthesis in microwave plasma torch at atmospheric pressure, *Mater. Sci. Eng., C*, 2006, **26**(5), 1189–1193.
47 P. Kaushik, *et al.*, *Carbon Nanotubes Grown by Microwave Torch for Ammonia Gas Detection.* 2016.
48 G. Z. Chen, *et al.*, Electrolytic conversion of graphite to carbon nanotubes in fused salts, *J. Electroanal. Chem.*, 1998, **446**(1), 1–6.
49 A. Peigney, *et al.*, A study of the formation of single-and double-walled carbon nanotubes by a CVD method, *J. Phys. Chem. B*, 2001, **105**(40), 9699–9710.
50 M. Kumar and Y. Ando, Chemical vapor deposition of carbon nanotubes: a review on growth mechanism and mass production, *J. Nanosci. Nanotechnol.*, 2010, **10**(6), 3739–3758.
51 M. Jung, *et al.*, Growth of carbon nanotubes by chemical vapor deposition, *Diamond Relat. Mater.*, 2001, **10**(3), 1235–1240.
52 C. Bower, *et al.*, Nucleation and growth of carbon nanotubes by microwave plasma chemical vapor deposition, *Appl. Phys. Lett.*, 2000, **77**(17), 2767–2769.
53 E. P. Favvas, *et al.*, High purity multi-walled carbon nanotubes: preparation, characterization and performance as filler materials in co-polyimide hollow fiber membranes, *Sep. Purif. Technol.*, 2014, **122**, 262–269.
54 J. Bernholc, C. Roland and B. I. Yakobson, Nanotubes, *Curr. Opin. Solid State Mater. Sci.*, 1997, **2**(6), 706–715.
55 Z. B. He, *et al.*, *Nickel catalyst faceting in plasma-enhanced direct current chemical vapor deposition of carbon nanofibers.* 2010.
56 M. Ge and K. Sattler, Vapor-condensation generation and STM analysis of fullerene tubes, *Science*, 1993, **260**(5107), 515–518.
57 K. Sattler, Scanning tunneling microscopy of carbon nanotubes and nanocones, *Carbon*, 1995, **33**(7), 915–920.
58 S. S. Shams, R. Zhang and J. Zhu, Graphene synthesis: a Review, *Mater. Sci.*, 2015, **33**(3), 566–578.
59 P. Ranjan, *et al.*, A Low-Cost Non-explosive Synthesis of Graphene Oxide for Scalable Applications, *Sci. Rep.*, 2018, **8**(1), 12007.
60 N. I. Zaaba, *et al.*, Synthesis of Graphene Oxide using Modified Hummers Method: Solvent Influence, *Procedia Eng.*, 2017, **184**, 469–477.
61 D. C. Marcano, *et al.*, Correction to Improved Synthesis of Graphene Oxide, *ACS Nano*, 2018, **12**(2), 2078.
62 J. Song, X. Wang and C.-T. Chang, Preparation and Characterization of Graphene Oxide, *J. Nanomater.*, 2014, **2014**, 276143.
63 Z. Hou, D. Xu and B. Cai, Ionization gas sensing in a microelectrode system with carbon nanotubes, *Appl. Phys. Lett.*, 2006, **89**(21), 213502.
64 H. Song, K. Li and Q. Li, A tripolar-electrode ionization gas sensor using a carbon nanotube cathode for NO detection, *J. Micromech. Microeng.*, 2018, **28**(6), 065010.
65 R. Tang, *et al.*, Carbon nanotube-based chemiresistive sensors, *Sensors*, 2017, **17**(4), 882.
66 M. Yoosefian, Powerful greenhouse gas nitrous oxide adsorption onto intrinsic and Pd doped Single walled carbon nanotube, *Appl. Surf. Sci.*, 2017, **392**, 225–230.
67 J. T. W. Yeow and J. P. M. She, Carbon nanotube-enhanced capillary condensation for a capacitive humidity sensor, *Nanotechnology*, 2006, **17**(21), 5441–5448.
68 W.-P. Chen, *et al.*, A capacitive humidity sensor based on multi-wall carbon nanotubes (MWCNTs), *Sensors*, 2009, **9**(9), 7431–7444.
69 S. Chopra, *et al.*, Selective gas detection using a carbon nanotube sensor, *Appl. Phys. Lett.*, 2003, **83**(11), 2280–2282.
70 C. Tasaltin and F. Basarir, Preparation of flexible VOC sensor based on carbon nanotubes and gold nanoparticles, *Sens. Actuators, B*, 2014, **194**, 173–179.
71 B. Philip, *et al.*, Carbon nanotube/PMMA composite thin films for gas-sensing applications, *Smart Mater. Struct.*, 2003, **12**(6), 935.
72 S. G. Chatterjee, *et al.*, Graphene–metal oxide nanohybrids for toxic gas sensor: A review, *Sens. Actuators, B*, 2015, **221**, 1170–1181.
73 S. Mun, Y. Chen and J. Kim, Cellulose–titanium dioxide–multiwalled carbon nanotube hybrid nanocomposite and its ammonia gas sensing properties at room temperature, *Sens. Actuators, B*, 2012, **171**, 1186–1191.
74 Y. Lin, *et al.*, Controllable synthesis of Co3O4/polyethyleneimine-carbon nanotubes nanocomposites for CO and NH3 gas sensing at room temperature, *J. Alloys Compd.*, 2015, **639**, 187–196.
75 S. Aslam, *et al.*, Graphene oxide coated graphene foam based chemical sensor, *Mater. Lett.*, 2019, **235**, 66–70.
76 K. Tamersit and F. Djeffal, Double-gate graphene nanoribbon field-effect transistor for DNA and gas sensing applications: simulation study and sensitivity analysis, *IEEE Sensor. J.*, 2016, **16**(11), 4180–4191.

77 R. Fang, *et al.*, The regulating role of carbon nanotubes and graphene in lithium-ion and lithium–sulfur batteries, *Adv. Mater.*, 2019, **31**(9), 1800863.
78 C. Li, *et al.*, Scalable self-propagating high-temperature synthesis of graphene for supercapacitors with superior power density and cyclic stability, *Adv. Mater.*, 2017, **29**(7), 1604690.
79 C. W. Foster, *et al.*, 3D printed graphene based energy storage devices, *Sci. Rep.*, 2017, **7**, 42233.
80 E. Campbell, *et al.*, Graphene oxide as a multifunctional platform for intracellular delivery, imaging, and cancer sensing, *Sci. Rep.*, 2019, **9**(1), 1–9.
81 G. Reina, *et al.*, Promises, facts and challenges for graphene in biomedical applications, *Chem. Soc. Rev.*, 2017, **46**(15), 4400–4416.
82 S. Kumar, *et al.*, ZnO-graphene quantum dots heterojunctions for natural sunlight-driven photocatalytic environmental remediation, *Appl. Surf. Sci.*, 2018, **447**, 802–815.
83 B. Raval and I. Banerjee, Functionalized Graphene Nanocomposite in Gas Sensing, in *Functionalized Graphene Nanocomposites and their Derivatives*. 2019, Elsevier. pp. 295–322.
84 F. Schedin, *et al.*, Detection of individual gas molecules adsorbed on graphene, *Nat. Mater.*, 2007, **6**(9), 652–655.
85 S. Tang and Z. Cao, Adsorption of nitrogen oxides on graphene and graphene oxides: insights from density functional calculations, *J. Chem. Phys.*, 2011, **134**(4), 044710.
86 M. Fathy, *et al.*, Optimizing the preparation parameters of GO and rGO for large-scale production, *J. Mater. Sci.*, 2016, **51**(12), 5664–5675.
87 W. Tian, X. Liu and W. Yu, Research progress of gas sensor based on graphene and its derivatives: a review, *Appl. Sci.*, 2018, **8**(7), 1118.
88 Y. Xia, *et al.*, 3D architectured graphene/metal oxide hybrids for gas sensors: A review, *Sensors*, 2018, **18**(5), 1456.
89 D. Sun, *et al.*, Graphene-enhanced metal oxide gas sensors at room temperature: a review, *Beilstein J. Nanotechnol.*, 2018, **9**(1), 2832–2844.
90 F.-L. Meng, Z. Guo and X.-J. Huang, Graphene-based hybrids for chemiresistive gas sensors, *Trac. Trends Anal. Chem.*, 2015, **68**, 37–47.
91 S. Prezioso, *et al.*, Graphene oxide as a practical solution to high sensitivity gas sensing, *J. Phys. Chem. C*, 2013, **117**(20), 10683–10690.
92 G. Lu, *et al.*, Toward practical gas sensing with highly reduced graphene oxide: a new signal processing method to circumvent run-to-run and device-to-device variations, *ACS Nano*, 2011, **5**(2), 1154–1164.
93 A. Lipatov, *et al.*, Highly selective gas sensor arrays based on thermally reduced graphene oxide, *Nanoscale*, 2013, **5**(12), 5426–5434.
94 T. Kawaguchi, *et al.*, Surface plasmon resonance immunosensor using Au nanoparticle for detection of TNT, *Sens. Actuators, B*, 2008, **133**(2), 467–472.
95 M. D. N. DobrokhotovV, M. G. Norton, A. Abuzir, W. J. Yeh and I. Stevenson, *Principles and mechanisms of gas sensing by GaN nanowires.* 2006, pp. 104302–104309.
96 M. G. Manera, J. Spadavecchia, D. Buso, C. de JuliánFernández, G. Mattei, A. Martucci, P. Mulvaney, J. Pérez-Juste, R. Rella, L. Vasanelli and P. Mazzoldi, Optical gas sensing of TiO2 and TiO2/Au nanocomposite thin films, *Sens. Actuators, B*, 2008, 107–115.
97 N. A. A. Borhaninia and N. Salehifar, Gas sensing properties of SnO2 nanoparticles mixed with gold nanoparticles, *Trans. Nonferrous Met. Soc. China*, 2017, 1777–1784.
98 H. T. Naama S, A. Keffous and G. Nezzal, CO2 gas sensorbased on silicon nanowires modified with metal nanoparticles, *Mater. Sci. Semicond. Process.*, 2015, 1369–8001.
99 A. M. Alwan and A. B. Dheyab, Room Temperature CO2 gas sensors of AuNPs/mesoPSi hybrid structures, *Appl. Nanosci.*, 2017, 335–341.
100 R. Lopez, E. Vigueras-Santiago, A. R. Vilchis-Nestor, V. H. Castrejon-Sanchez, A. A. Lopez and N. Torres-Gomez, Ether gas -sensor based on Au nanoparticle decorated ZnO microstructure, *Results Phys.*, 2017, 1818–1823.
101 L. Wang, S. Wang, M. Xu, X. Hu, H. Zhang, Y. Wang and W. Huang, A Au-functionalized ZnO nanowire gas sensor for detection of benzene and toluene, *Phys. Chem. Chem. Phys.*, 2013, 17179–17186.
102 L. Tabrizi and H. Chiniforoshan, High-performance room temperature gas sensor based on gold (III) pincer complex with high sensitivity for NH3, *Sens. Actuators, B*, 2017, **245**, 815–820.
103 J. Zhang, *et al.*, High-Performance Ketone Sensing in Vapor Phase Enabled by o-Carborane-Modified Cyclometalated Alkynyl-Gold (III) Complex-Based Fluorescent Films, *ACS Appl. Mater. Interfaces*, 2021.
104 S. V. Ganachari, D. Raghunandan, R. Bhat, N. V. S. Rao, D. S. Huh and A. Venkataraman, Gas sensing characteristic of biofunctionalized gold nanoparticles, *J. Bionanosci.*, 2011, 107–112.
105 Y. Ma and L. Y. L. Yung, Detection of dissolved CO2 based on aggregation of gold nanoparticles, *Anal. Chem.*, 2014, 2429–2435.
106 Z. Xie, R. R. M. V., A. C. Stewart, M. H. Nantz and X.-N. Fu, Imparting sensitivity and selectivity to a gold nanoparticle chemiresistor through thiol monolayer functionalization for sensing acetone. *RSC Adv.*, 35618–35624.
107 D. R. Daskal Y, J. Walter and Y. Joseph, *Chemiresistor sensor based on gold nanoparticle composites*, Procedia Engineering, 2015, pp. 799–802.
108 Y.-T. W. Tian-Li Han, J.-J. Li, H.-G. Zhang, J.-H. Liu and X.-J. Huang, In situ gold nanoparticle-decorated three-dimensional tin dioxide gas-sensing detection of volatile organic compounds, *J. Mater. Chem. C*, 2017, 6193–6201.
109 Y. Fang, *et al.*, Sensitivity enhancement of flexible gas sensors *via* conversion of inkjet-printed silver electrodes into porous gold counterparts, *Sci. Rep.*, 2017, **7**(1), 8988.
110 H.-R. Lim, *et al.*, All-in-one, wireless, fully flexible sodium sensor system with integrated Au/CNT/Au nanocomposites, *Sens. Actuators, B*, 2021, **331**, 129416.

111 T. Lu, E. M. Goldfield and S. K. Gray, Quantum States of Hydrogen and Its Isotopes Confined in Single-Walled Carbon Nanotubes: Dependence on Interaction Potential and Extreme Two-Dimensional Confinement, *J. Phys. Chem. B*, 2006, **110**(4), 1742–1751.

112 M. Ashino, *et al.*, Atomically resolved mechanical response of individual metallofullerene molecules confined inside carbon nanotubes, *Nat. Nanotechnol.*, 2008, **3**, 337.

113 L. Jiang and L. Gao, Modified carbon nanotubes: an effective way to selective attachment of gold nanoparticles, *Carbon*, 2003, **41**(15), 2923–2929.

114 A. La Torre, *et al.*, Transport and encapsulation of gold nanoparticles in carbon nanotubes, *Nanoscale*, 2010, **2**(6), 1006–1010.

115 R. Zanella, *et al.*, Deposition of gold nanoparticles onto thiol-functionalized multiwalled carbon nanotubes, *J. Phys. Chem. B*, 2005, **109**(34), 16290–16295.

116 B. Kim and W. M. Sigmund, Functionalized multiwall carbon nanotube/gold nanoparticle composites, *Langmuir*, 2004, **20**(19), 8239–8242.

117 K. Balasubramanian, *et al.*, A Selective Electrochemical Approach to Carbon Nanotube Field-Effect Transistors, *Nano Lett.*, 2004, **4**(5), 827–830.

118 R. J. Chen, *et al.*, Noncovalent Sidewall Functionalization of Single-Walled Carbon Nanotubes for Protein Immobilization, *J. Am. Chem. Soc.*, 2001, **123**(16), 3838–3839.

119 M. S. Raghuveer, *et al.*, Microwave-assisted single-step functionalization and in situ derivatization of carbon nanotubes with gold nanoparticles, *Chem. Mater.*, 2006, **18**(6), 1390–1393.

120 D. Gingery and P. Bühlmann, Formation of gold nanoparticles on multiwalled carbon nanotubes by thermal evaporation, *Carbon*, 2008, **46**(14), 1966–1972.

121 A. Felten, C. Bittencourt and J.-J. Pireaux, Gold clusters on oxygen plasma functionalized carbon nanotubes: XPS and TEM studies, *Nanotechnology*, 2006, **17**(8), 1954.

122 H. C. Choi, *et al.*, Spontaneous Reduction of Metal Ions on the Sidewalls of Carbon Nanotubes, *J. Am. Chem. Soc.*, 2002, **124**(31), 9058–9059.

123 D. S. Kim, T. Lee and K. E. Geckeler, Hole-Doped Single-Walled Carbon Nanotubes: Ornamenting with Gold Nanoparticles in Water, *Angew. Chem., Int. Ed.*, 2006, **45**(1), 104–107.

124 Y. Zhang, *et al.*, Metal coating on suspended carbon nanotubes and its implication to metal–tube interaction, *Chem. Phys. Lett.*, 2000, **331**(1), 35–41.

125 A. Tello, *et al.*, The synthesis of hybrid nanostructures of gold nanoparticles and carbon nanotubes and their transformation to solid carbon nanorods, *Carbon*, 2008, **46**(6), 884–889.

126 R. Gao and J. Zheng, Amine-terminated ionic liquid functionalized carbon nanotube-gold nanoparticles for investigating the direct electron transfer of glucose oxidase, *Electrochem. Commun.*, 2009, **11**(3), 608–611.

127 H. Xu, *et al.*, Microwave-radiated synthesis of gold nanoparticles/carbon nanotubes composites and its application to voltammetric detection of trace mercury (II), *Electrochem. Commun.*, 2008, **10**(12), 1839–1843.

128 Y. Shi, R. Yang and P. K. Yuet, Easy decoration of carbon nanotubes with well dispersed gold nanoparticles and the use of the material as an electrocatalyst, *Carbon*, 2009, **47**(4), 1146–1151.

129 K. S. Coleman, *et al.*, Functionalization of Single-Walled Carbon Nanotubes *via* the Bingel Reaction, *J. Am. Chem. Soc.*, 2003, **125**(29), 8722–8723.

130 J. Shi, Z. Wang and H.-l. Li, Selfassembly of gold nanoparticles onto the surface of multiwall carbon nanotubes functionalized with mercaptobenzene moieties, *J. Nanoparticle Res.*, 2006, **8**(5), 743–747.

131 B. He and G. Du, Novel electrochemical aptasensor for ultrasensitive detection of sulfadimidine based on covalently linked multi-walled carbon nanotubes and in situ synthesized gold nanoparticle composites, *Anal. Bioanal. Chem.*, 2018, **410**(12), 2901–2910.

132 D. Rao, Q. Sheng and J. Zheng, Self-assembly preparation of gold nanoparticle decorated 1-pyrenemethylamine functionalized graphene oxide–carbon nanotube composites for highly sensitive detection of nitrite, *Anal. Methods*, 2016, **8**(24), 4926–4933.

133 M. Zhang, L. Su and L. Mao, Surfactant functionalization of carbon nanotubes (CNTs) for layer-by-layer assembling of CNT multi-layer films and fabrication of gold nanoparticle/CNT nanohybrid, *Carbon*, 2006, **44**(2), 276–283.

134 M. Amatatongchai, *et al.*, Simple flow injection for determination of sulfite by amperometric detection using glassy carbon electrode modified with carbon nanotubes–PDDA–gold nanoparticles, *Talanta*, 2015, **133**, 134–141.

135 V. D. Chinh, *et al.*, Synthesis of gold nanoparticles decorated with multiwalled carbon nanotubes (Au-MWCNTs) *via* cysteaminium chloride functionalization, *Sci. Rep.*, 2019, **9**(1), 5667.

136 R. Shevate, *et al.*, Embedding 1D Conducting Channels into 3D Isoporous Polymer Films for High-Performance Humidity, *Sensing*, 2018, **57**(35), 11218–11222.

137 Z. P. Michael, *et al.*, Probing Biomolecular Interactions with Gold Nanoparticle-Decorated Single-Walled Carbon Nanotubes, *J. Phys. Chem. C*, 2017, **121**(38), 20813–20820.

138 R. Burgess, *et al.*, The functionalisation of graphite surfaces with nitric acid: Identification of functional groups and their effects on gold deposition, *J. Catal.*, 2015, **323**, 10–18.

139 J. C. Charlier, *et al.*, Carbon nanotubes randomly decorated with gold clusters: from nano2hybrid atomic structures to gas sensing prototypes, *Nanotechnology*, 2009, **20**(37), 375501.

140 V. Duc Chinh, *et al.*, Synthesis of Gold Nanoparticles Decorated with Multiwalled Carbon Nanotubes (Au-MWCNTs) *via* Cysteaminium Chloride Functionalization, *Sci. Rep.*, 2019, **9**(1), 5667.

141 K. Kardimi, *et al.*, Synthesis and characterization of carbon nanotubes decorated with Pt and PtRu nanoparticles and assessment of their electrocatalytic performance, *Int. J. Hydrogen Energy*, 2012, **37**(2), 1243–1253.

142 J. Zhang, *et al.*, Nanostructured materials for room-temperature gas sensors, *Adv. Mater.*, 2016, **28**(5), 795–831.
143 S. Abdulla, T. L. Mathew and B. Pullithadathil, Highly sensitive, room temperature gas sensor based on polyaniline-multiwalled carbon nanotubes (PANI/MWCNTs) nanocomposite for trace-level ammonia detection, *Sens. Actuators, B*, 2015, **221**, 1523–1534.
144 N. Kumar, P. Sahatiya and P. Dubey, Fabrication of CNT based Gas Sensor Using Interdigitated Gold Electrodes, *Procedia Mater. Sci.*, 2014, **6**, 1976–1980.
145 S.-J. Young, *et al.*, Ethanol gas sensors composed of carbon nanotubes with adsorbed gold nanoparticles, *Int. J. Electrochem. Sci.*, 2012, **7**(11), 11634–11640.
146 Z.-D. Lin, *et al.*, Carbon nanotubes with adsorbed Au for sensing gas, *IEEE Sensor. J.*, 2013, **13**(6), 2423–2427.
147 K. Lee, *et al.*, Highly sensitive, transparent, and flexible gas sensors based on gold nanoparticle decorated carbon nanotubes, *Sens. Actuators, B*, 2013, **188**, 571–575.
148 R. Bogue, Recent developments in MEMS sensors: A review of applications, markets and technologies, *Sens. Rev.*, 2013.
149 M. Erfan, *et al.*, On-chip micro–electro–mechanical system Fourier transform infrared (MEMS FT-IR) spectrometer-based gas sensing, *Appl. Spectrosc.*, 2016, **70**(5), 897–904.
150 D. Im, *et al.*, Improved formaldehyde gas sensing properties of well-controlled Au nanoparticle-decorated In2O3 nanofibers integrated on low power MEMS platform, *J. Mater. Sci. Technol.*, 2020, **38**, 56–63.
151 Y. Wang, *et al.*, Sputtered SnO2: NiO thin films on self-assembled Au nanoparticle arrays for MEMS compatible NO2 gas sensors, *Sens. Actuators, B*, 2019, **278**, 28–38.
152 Y. Nagarjuna and Y.-J. Hsiao, Au Doping ZnO Nanosheets Sensing Properties of Ethanol Gas Prepared on MEMS Device, *Coatings*, 2020, **10**(10), 945.
153 X. Zang, *et al.*, Graphene and carbon nanotube (CNT) in MEMS/NEMS applications, *Microelectron. Eng.*, 2015, **132**, 192–206.
154 J. Lee, *et al.*, MEMS gas preconcentrator filled with CNT foam for exhaled VOC gas detection, *BioChip J.*, 2015, **9**(1), 44–49.
155 Z. Hou, *et al.*, A MEMS-Based Ionization Gas Sensor Using Carbon Nanotubes, *IEEE Trans. Electron Devices*, 2007, **54**(6), 1545–1548.
156 B. Sharma, H. Yadav and J.-S. Kim, MEMS based hydrogen sensor with the highly porous Au-CNT film as a sensing material, *J. Mater. Sci.: Mater. Electron.*, 2017, **28**(18), 13540–13547.
157 M. Penza, *et al.*, Functional characterization of carbon nanotube networked films functionalized with tuned loading of Au nanoclusters for gas sensing applications, *Sens. Actuators, B*, 2009, **140**(1), 176–184.
158 E. Dilonardo, *et al.*, Enhancement of the gas sensing performance of carbon nanotube networked films based on their electrophoretic functionalization with gold nanoparticles, *MRS Online Proc. Libr.*, 2015, **1786**, 37–42.
159 P. R. Mudimela, *et al.*, Gas sensing with gold-decorated vertically aligned carbon nanotubes, *Beilstein J. Nanotechnol.*, 2014, **5**(1), 910–918.
160 J. Lee, *et al.*, Magnetically Aligned Iron Oxide/Gold Nanoparticle-Decorated Carbon Nanotube Hybrid Structure as a Humidity Sensor, *ACS Appl. Mater. Interfaces*, 2015, **7**(28), 15506–15513.
161 A. Thamri, *et al.*, MHDA-Functionalized Multiwall Carbon Nanotubes for detecting non-aromatic VOCs, *Sci. Rep.*, 2016, **6**, 35130.
162 A. Abdelghani, *et al.*, Study of self-assembled monolayers of n-alkanethiol on a surface plasmon resonance fibre optic sensor, *Thin Solid Films*, 1996, **284**, 157–161.
163 F. Wang and T. M. Swager, Diverse Chemiresistors Based upon Covalently Modified Multiwalled Carbon Nanotubes, *J. Am. Chem. Soc.*, 2011, **133**(29), 11181–11193.
164 E. Frontera, *et al.*, Tuning the molecular sensitivity of conductive polymer resistive sensors by chemical functionalization. in *Key Engineering Materials*, Trans Tech Publ, 2014.
165 M. Brust, *et al.*, Synthesis of thiol-derivatised gold nanoparticles in a two-phase Liquid–Liquid system, *J. Chem. Soc., Chem. Commun.*, 1994, (7), 801–802.
166 S. T. Hasnahena and M. Roy, Sensing of low concentration of ammonia at room temperature by decorated multi-walled carbon nanotube: fabrication and characteristics, *Appl. Phys. A: Solids Surf.*, 2017, **124**(1), 4.
167 P. Clément, *et al.*, Deep Cavitand Self-Assembled on Au NPs-MWCNT as Highly Sensitive Benzene Sensing Interface, *Adv. Funct. Mater.*, 2015, **25**(26), 4011–4020.
168 Z. Zanolli, *et al.*, Gas Sensing with Au-Decorated Carbon Nanotubes, *ACS Nano*, 2011, **5**(6), 4592–4599.
169 D. M. Rudkevich, G. Hilmersson and J. Rebek, Self-Folding Cavitands, *J. Am. Chem. Soc.*, 1998, **120**(47), 12216–12225.
170 M. Ding, *et al.*, Welding of Gold Nanoparticles on Graphitic Templates for Chemical Sensing, *J. Am. Chem. Soc.*, 2012, **134**(7), 3472–3479.
171 Y. Wu and P. Yang, Melting and Welding Semiconductor Nanowires in Nanotubes, *Adv. Mater.*, 2001, **13**(7), 520–523.
172 F. Lasserre, *et al.*, Simultaneous deposition of carbon nanotubes and decoration with gold–palladium nanoparticles by laser-induced forward transfer, *Appl. Phys. A: Solids Surf.*, 2016, **122**(3), 150.
173 N. Gogurla, *et al.*, Multifunctional Au-ZnO plasmonic nanostructures for enhanced UV photodetector and room temperature NO sensing devices, *Sci. Rep.*, 2014, **4**, 6483.
174 M. Quintana, *et al.*, Light-Induced Selective Deposition of Au Nanoparticles on Single-Wall Carbon Nanotubes, *ACS Nano*, 2010, **4**(10), 6105–6113.
175 M. Angiola, *et al.*, Transparent carbon nanotube film as sensitive material for surface plasmon resonance based optical sensors, *Sens. Actuators, B*, 2016, **236**, 1098–1103.
176 F. Sajed and C. Rutherglen, All-printed and transparent single walled carbon nanotube thin film transistor devices, *Appl. Phys. Lett.*, 2013, **103**(14), 185_1.

177 M. Y. Lone, *et al.*, Enhancement of sensor response of as fabricated SWCNT sensor with gold decorated nanoparticles, *Sens. Actuators, A*, 2018, **274**, 85–93.
178 Z. Lin, S. Young and S. Chang, Carbon Nanotube Thin Films Functionalized *via* Loading of Au Nanoclusters for Flexible Gas Sensors Devices, *IEEE Trans. Electron Devices*, 2016, **63**(1), 476–480.
179 S. Young and Z. Lin, Ammonia gas sensors with Au-decorated carbon nanotubes, *Microsyst. Technol.*, 2018, **24**(10), 4207–4210.
180 E. G. Bakhoum and M. H. Cheng, Miniature carbon monoxide detector based on nanotechnology, *IEEE Trans. Instrum. Meas.*, 2012, **62**(1), 240–245.
181 S. Freddi, *et al.*, Enhanced selectivity of target gas molecules through a minimal array of gas sensors based on nanoparticle-decorated SWCNTs, *Analyst*, 2019, **144**(13), 4100–4110.
182 Q. Chang, *et al.*, Preparation of gold/polyaniline/multiwall carbon nanotube nanocomposites and application in ammonia gas detection, *J. Mater. Sci.*, 2008, **43**(17), 5861–5866.
183 S.-W. Choi, *et al.*, Remarkable improvement of CO-sensing performances in single-walled carbon nanotubes due to modification of the conducting channel by functionalization of Au nanoparticles, *Sens. Actuators, B*, 2016, **232**, 625–632.
184 T. P. McNicholas, *et al.*, Sensitive Detection of Elemental Mercury Vapor by Gold-Nanoparticle-Decorated Carbon Nanotube Sensors, *J. Phys. Chem. C*, 2011, **115**(28), 13927–13931.
185 M. Gautam and A. H. Jayatissa, Ammonia gas sensing behavior of graphene surface decorated with gold nanoparticles, *Solid-State Electron.*, 2012, **78**, 159–165.
186 Y. Zhou, *et al.*, UV Illumination-enhanced molecular ammonia detection based on a ternary-reduced graphene oxide–titanium dioxide–Au composite film at room temperature, *Anal. Chem.*, 2018, **91**(5), 3311–3318.
187 Q. A. Drmosh, *et al.*, UV-activated gold decorated rGO/ZnO heterostructured nanocomposite sensor for efficient room temperature H2 detection, *Sens. Actuators, B*, 2019, **290**, 666–675.
188 R. Peng, *et al.*, Boron-doped graphene coated Au@ SnO2 for high-performance triethylamine gas detection, *Mater. Chem. Phys.*, 2020, **239**, 121961.
189 Y. Zhang, *et al.*, Confinement preparation of Au nanoparticles embedded in ZIF-67-derived N-doped porous carbon for high-performance detection of hydrazine in liquid/gas phase, *Sens. Actuators, B*, 2019, **285**, 607–616.
190 H. Wan, *et al.*, High sensitive reduced graphene oxide-based room temperature ionic liquid electrochemical gas sensor with carbon-gold nanocomposites amplification, *Sens. Actuators, B*, 2019, **299**, 126952.
191 P. Seifaddini, *et al.*, Room temperature ammonia gas sensor based on Au/graphene nanoribbon, *Mater. Res. Express*, 2019, **6**(4), 045054.
192 G. V. Kamarchuk, *et al.*, New chemical sensors based on point heterocontact between single wall carbon nanotubes and gold wires, *Sens. Actuators, B*, 2008, **134**(2), 1022–1026.
193 G. Kamarchuk, *et al.*, Point-contact sensors: New prospects for a nanoscale-sensitive technique, *Europhys. Lett.*, 2006, **76**(4), 575.
194 M. Itkis, *et al.*, Spectroscopic study of the Fermi level electronic structure of single-walled carbon nanotubes, *Nano Lett.*, 2002, **2**(2), 155–159.
195 C. Y. Lee, *et al.*, Charge transfer from metallic single-walled carbon nanotube sensor arrays, *J. Phys. Chem. B*, 2006, **110**(23), 11055–11061.
196 D. R. Kauffman, *et al.*, Understanding the sensor response of metal-decorated carbon nanotubes, *Nano Lett.*, 2010, **10**(3), 958–963.
197 D. R. Kauffman and A. Star, Chemically induced potential barriers at the carbon nanotube– metal nanoparticle interface, *Nano Lett.*, 2007, **7**(7), 1863–1868.
198 S. Link, *et al.*, Electron dynamics in gold and gold–silver alloy nanoparticles: The influence of a nonequilibrium electron distribution and the size dependence of the electron–phonon relaxation, *J. Chem. Phys.*, 1999, **111**(3), 1255–1264.
199 P. E. Hopkins, J. L. Kassebaum and P. M. Norris, Effects of electron scattering at metal-nonmetal interfaces on electron-phonon equilibration in gold films, *J. Appl. Phys.*, 2009, **105**(2), 023710.
200 D. R. Kauffman and A. Star, Carbon nanotube gas and vapor sensors, *Angew. Chem., Int. Ed.*, 2008, **47**(35), 6550–6570.
201 Z. A. Page, V. V. Duzhko and T. Emrick, Conjugated thiophene-containing polymer zwitterions: Direct synthesis and thin film electronic properties, *Macromolecules*, 2012, **46**(2), 344–351.
202 P. Liu, *et al.*, Measuring the work function of carbon nanotubes with thermionic method, *Nano Lett.*, 2008, **8**(2), 647–651.
203 G. Lu, L. E. Ocola and J. Chen, Room-temperature gas sensing based on electron transfer between discrete tin oxide nanocrystals and multiwalled carbon nanotubes, *Adv. Mater.*, 2009, **21**(24), 2487–2491.
204 Y. Liu, *et al.*, Mesoporous Co3O4-supported gold nanocatalysts: Highly active for the oxidation of carbon monoxide, benzene, toluene, and o-xylene, *J. Catal.*, 2014, **309**, 408–418.
205 H. Chu, *et al.*, Decoration of gold nanoparticles on surface-grown single-walled carbon nanotubes for detection of every nanotube by surface-enhanced Raman spectroscopy, *J. Am. Chem. Soc.*, 2009, **131**(40), 14310–14316.
206 L. Beqa, *et al.*, Chemically attached gold nanoparticle–carbon nanotube hybrids for highly sensitive SERS substrate, *Chem. Phys. Lett.*, 2011, **512**(4–6), 237–242.
207 K. Chung, *et al.*, Systematic Study on the Sensitivity Enhancement in Graphene Plasmonic Sensors Based on Layer-by-Layer Self-Assembled Graphene Oxide

Multilayers and Their Reduced Analogues, *ACS Appl. Mater. Interfaces*, 2015, **7**(1), 144–151.

208 Q. Xi, *et al.*, Gold Nanoparticle-Embedded Porous Graphene Thin Films Fabricated *via* Layer-by-Layer Self-Assembly and Subsequent Thermal Annealing for Electrochemical Sensing, *Langmuir*, 2012, **28**(25), 9885–9892.

209 R. Furue, *et al.*, Arsine gas sensor based on gold-modified reduced graphene oxide, *Sens. Actuators, B*, 2017, **240**, 657–663.

210 G. Goncalves, *et al.*, Surface modification of graphene nanosheets with gold nanoparticles: the role of oxygen moieties at graphene surface on gold nucleation and growth, *Chem. Mater.*, 2009, **21**(20), 4796–4802.

211 J. L. Johnson, *et al.*, Experimental study of graphitic nanoribbon films for ammonia sensing, *J. Appl. Phys.*, 2011, **109**(12), 124301.

212 G. Lee, *et al.*, Defect-engineered graphene chemical sensors with ultrahigh sensitivity, *Phys. Chem. Chem. Phys.*, 2016, **18**(21), 14198–14204.

213 L. Wang, *et al.*, Boron-Doped Graphene: Scalable and Tunable p-Type Carrier Concentration Doping, *J. Phys. Chem. C*, 2013, **117**(44), 23251–23257.